Molecular Imaging in Neurology and Psychiatry

16

The brain is the last and grandest biological frontier, the most complex thing we have yet discovered in our universe. It contains hundreds of billions of cells interlinked through trillions of connections. The brain boggles the mind.

James D. Watson

16.1 Neuroscience

16.1.1 The Nervous System

The nervous system is traditionally divided into central and peripheral components. The *central nervous system* (CNS) comprises the brain (cerebrum, cerebellum and brain stem) and spinal cord. The *peripheral nervous system* (PNS) includes sensory neurons and motor neurons, which connect CNS to sensory receptors and muscles, and glands, respectively. In the PNS, the *somatic* division innervates the skeletal muscles, while the autonomic (sympathetic and parasympathetic) division innervates smooth muscles, cardiac muscle, and glands. In the PNS, *ganglia* are accumulations of nerve cell bodies and their supporting cells, while *nerves* are bundles of nerve cell axons and their supporting cells.

16.1.2 Nerve Cells

The cells of the nervous system can be divided into two broad categories: nerve cells or *neurons* and a variety of supporting cells, which consist mostly of *neuroglial cells–referred to simply as glial cells or glia (*from the Greek word meaning glue).

The structure of neurons (Fig. 16.1) in many respects resembles that of most other cells in the body. The neuron has a cell body (containing a nucleus, mitochondria, etc.) and specialized extensions (for intercellular communication and signaling), known as dendites and axon. Dendritic branches or processes are specialized for receiving information from other cells, while the axon is designed for signal conduction. Since the fundamental purpose of neurons is to integrate information from other neurons, the number of inputs received by each neuron in the human nervous system ranges from 1 to approximately 100,000. Some neurons transmit locally, while others may carry signals several feet away from the cell body.

The glial cells are quite different from neurons; they do not participate directly in electrical signaling. Also, there may be three times more glial cells than neurons and these cells are usually smaller, and lack dendrites and axons. The main role played by glia includes maintaining the ionic milieu of nerve cells, modulating the rate of nerve signal propagation/synaptic action, and aiding in the recovery from neural injury. The three types of glia are *astrocytes*, *oligodendrocytes*, and *microglia*. Astrocytes maintain the appropriate chemical environment for neuronal signaling. Oligodendrocytes provide a wrapping (*myelin*) around some axons to increase the speed of signal conduction. Microglia, derived from hematopoietic stem cells, are similar in some ways to macrophages and help repair neural damage.

Neurons are organized into ensembles called circuits that process specific kinds of information. Neurons that carry information towards the CNS are called *afferent neurons*, while the neurons that carry information away from the CNS, are called *efferent neurons*.

S. Vallabhajosula, *Molecular Imaging: Radiopharmaceuticals for PET and SPECT,*
DOI: 10.1007/978-3-540-76735-0_16, © Springer-Verlag Berlin Heidelberg 2009

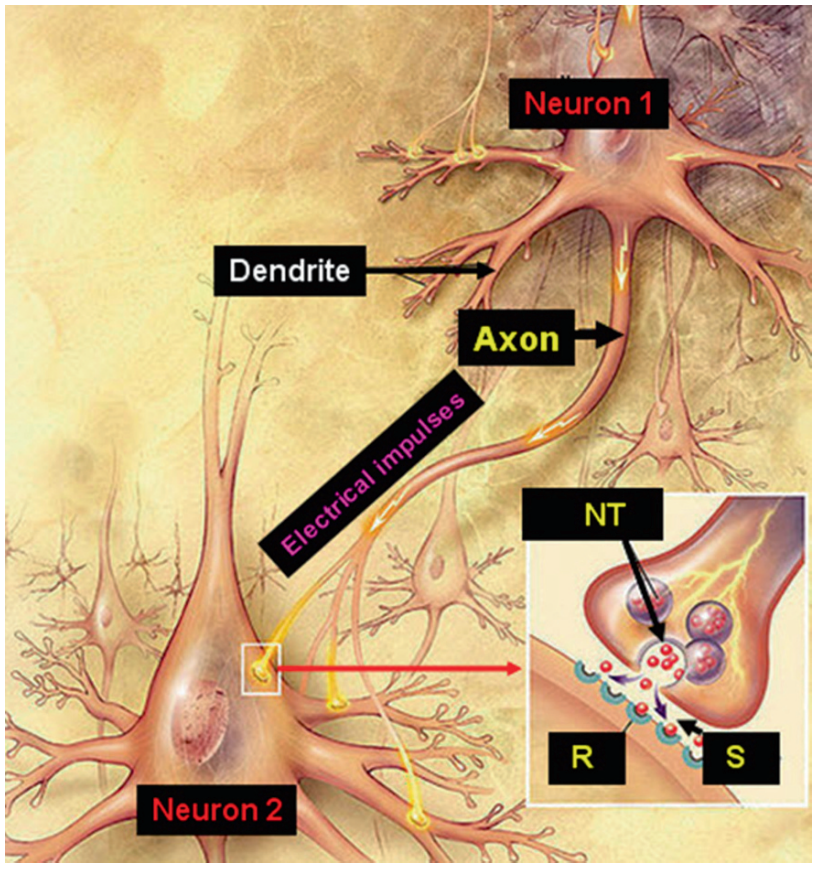

Fig. 16.1 The structure of a neuron with a cell body, dendrites, and the axon. The nerve signals transmitted along the axon trigger the release of neurotransmitter molecules into the synapse, the point of contact between two neurons or between a neuron and a target cell (modified from image at WordPress.com weblog)

Neurons that participate only in the local circuits are called interneurons. Sensory circuits provide information about the internal and external environment, while motor circuits respond to sensory inputs by generating movement.

16.1.3 The Human Brain

The CNS includes the brain and the spinal cord. The human brain (Fig. 16.2) consists of approximately 10,000 different types of neurons and a total of 100 billion neurons, and the adult brain weighs nearly 1,400 g. The brain is subdivided into three main regions: the *forebrain*, *midbrain* and *hind brain*. Collectively, the midbrain and hind brain are called the

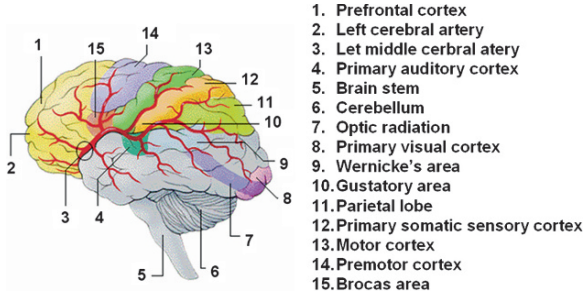

Fig. 16.2 The human brain showing the main lobes and major blood vessels

brain stem. The hindbrain has three principal subdivisions: the medulla oblongata, the cerebellum and the pons. The hindbrain tends to pass information to and receive controlling signals from the midbrain, which is itself controlled by the forebrain. The midbrain receives

and processes sensory information and distributes it to different parts of the forebrain for further processing. The forebrain integrates sensory information of various kinds and formulates motor commands that are executed by other parts of the CNS.

The forebrain is subdivided into the diencephalon (thalamus and hypothalamus) and telencephalon (the cerebrum and basal ganglia). The thalamus is a sensory relay station that distributes sensory information to appropriate regions in the cerebral cortex, while the hypothalamus maintains homeostasis. The cerebral cortex is the outer layer of the cerebrum (the two cerebral hemispheres) which contains most of the neurons and occupies a large convoluted surface area. The ridges are known as *gyri*, and the valleys are called *sulci* or *fissues*. The cerebral cortex is involved in the complex processing of sensory information to form perceptions, in the planning and initiation of movements, and in associative learning and higher cognition.

Each cerebral hemisphere is conventionally divided into four lobes (Fig. 16.3): the frontal, parietal, temporal, and occipital lobes. In addition to their role in primary and sensory processing, each lobe has characteristic cognitive functions. The frontal lobe is critical in planning behavior, the parietal lobe in attending to important stimuli, the temporal lobe in recognizing objects and faces, and the occipital lobe in a variety of visual analyses. The hippocampus, a highly specialized cortical structure that is folded into the medial temporal lobe plays a major role in memory.

When the brain is dissected, sectioned, or observed with noninvasive imaging techniques (CT, MRI, PET, SPECT), many deeper structures are apparent. Most of the cerebral cortex is made up of six layers and is referred to as neocortex. The *gray matter* refers to the cortex, whether cerebral, cerebellar, or hippocampal and is mainly made up of neuronal cell bodies, their dendrites, the axon terminals, and glia. The *white matter* makes up a large part of the subcortical tissue consisting mostly of axons entering or leaving the cortex. Among the internal structures, the *basal ganglia* play a major role in the organization and guidance of complex motor functions. The basal ganglia include the *striatum* (the *caudate* and the *putamen*) and the *globus pallidus*. Another important nucleus (collection of neurons) is the *amygdala*, which plays an important role in the emotional behavior.

The different parts of the cerebral hemispheres are interconnected by three large bundles of axons: the *corpus callosum*, *anterior commissure*, and *fornix*. The ventricular system in the CNS is a series of interconnected, fluid-filled spaces in the core of the forebrain and brain stem. The *cerebrospinal fluid* (CSF), produced by the choroid plexus, a network of specialized secretory tissue in the lateral, third, and fourth ventricles, percolates through the ventricular system into the *subarachnoid space*, which helps cushion the brain within the cranial cavity.

16.1.3.1 The Blood–Brain Barrier

The brain receives blood from two sources: the internal carotid arteries (ICA) and the vertebral arteries (VA). Many branches arising from ICA and VA supply blood to the brain and all the internal structures.

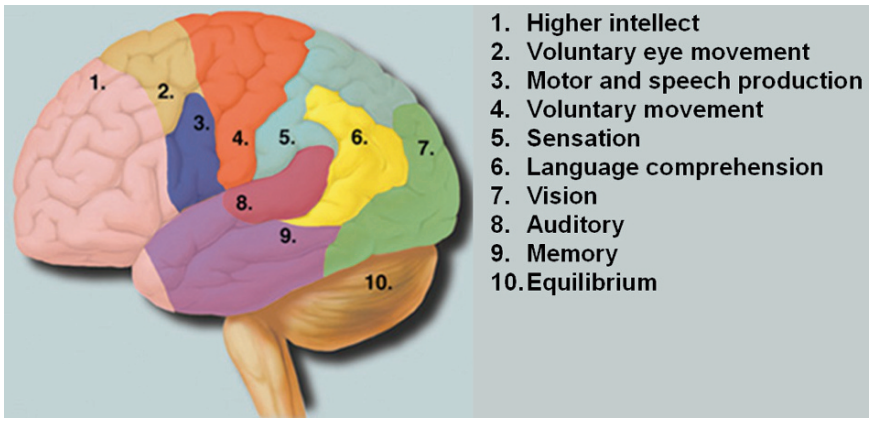

Fig. 16.3 The human brain showing the specific cortical areas associated with major functions

The blood supply of the brain is particularly significant because neurons are very sensitive to oxygen deprivation. The brain, more than any other organ, must be carefully shielded from toxic molecules and ionic species that would adversely affect the neuronal function. The interface between the walls of capillaries and the surrounding tissue is very important for the transport of various molecules and nutrients from the blood into the cells. In the brain, this interface has been given the special name, blood–brain barrier (BBB), since it protects and maintains homeostasis. Unlike in many other tissues, the adjacent capillary endothelial cells in the brain have very tight junctions, permitting the transport of molecules and ions, which can only move through the walls of the endothelial cell membranes. In addition to the tight junctions, the terminal regions of the astrocytic processes surround the outside of the capillary endothelial cells. As a result, only the neutral molecules that are lipid soluble (lipophilic) and molecules needed for cellular metabolism (such as glucose) that can be transported by facilitated diffusion are permitted to enter the brain tissue. Therefore, BBB presents a significant challenge in the development of molecular imaging probes to assess brain function (Chap. 9).

16.1.4 Neural Signaling

Neurons have evolved as a sophisticated means of generating electrical signals to convey information over long distances and transmit the signal to other cells. Ion pumps and ion channels on the cell membrane create substantial transmembrane gradients for most ions and are responsible for ionic movements across the cell membrane. In general, there are many more K^+ inside the neuron than outside, and many more Na^+ outside the neuron than inside. As a result, generally, neurons generate a negative potential, called the *resting membrane potential* (RMP), which typically is a fraction of a volt, −40 to −90 mV. An increase in the external K^+ concentration makes the RMP more positive. *Action potentials* represent transient changes in the RMP of neurons. An action potential (AP) is generated when a transient rise in Na^+ permeability allows a net flow of Na^+ across the membrane. As a result, the Na^+ is much more inside the neuron than outside. This influx of Na^+ represents passing an electrical current across membrane. *Depolarization* occurs when the membrane potential is more positive than the RMP. The brief period of depolarization is quickly followed by an increase in K^+ permeability that repolarizes the membrane and produces a brief undershoot of the AP. The membrane potential soon returns to the RMP. It is important to recognize that the membrane is depolarized in an all-or-none fashion. APs are propagated along the length of the axons and are the fundamental electrical signals of neurons.

16.1.5 Synaptic Transmission

The point at which a signal or activity is transmitted from one nerve cell to another, or from a motor neuron to a muscle cell is called a *synapse*. Synapses are classified into two general groups: electrical synapses and chemical synapses. In both types, the input cell, called the *presynaptic cell* comes into contact with the output cell, called the *postsynaptic cell*.

In an electrical synapse, the membranes of the two communicating neurons are usually close together, and are linked by a special kind of intercellular contact called a gap junction, which contains precisely aligned paired channels in the membrane of each neuron. The pores of the channels connect to one another allowing the exchange of ions and small molecules (such as ATP and second messengers). The gap junction permits the current to flow passively from the presynaptic neuron, and initiates or inhibits the generation of a postsynaptic membrane potential. Hormone-secreting neurons within the hypothalamus communicate through gap junctions.

16.1.5.1 Chemical Synapses

A generalized structure of a chemical synapse is shown in Fig. 16.6 The separation between the presynaptic and postsynaptic neurons is called the synaptic cleft. Transmission between the two neurons is on the basis of special molecules called neurotransmitters. The sequence of events involved in the chemical neurotransmission at a synapse is as follows:

- In the presynaptic neuron, the neurotransmitter molecules are synthesized and stored in the vesicles.

- An action potential reaching the presynaptic neuron terminal causes the opening of voltage gated Ca^{2+} channels.
- The influx of Ca^{2+} causes vesicles to fuse with presynaptic membrane.
- The neurotransmitter molecules are released into the synaptic cleft via exocytosis.
- The transmitter binds to specific receptors on the membrane of a postsynaptic neuron leading to (a) change in ionic permeability of postsynaptic neuron or (b) an intracellular release or production of a second messenger, which in turn interacts directly or indirectly with an ion channel, causing it to open or close.
- The postsynaptic current generated by the change in permeability of ions changes the membrane potential.
- The potential changes that increase the probability of firing an action potential are called excitatory, whereas those that decrease the probability of firing an action potential are called inhibitory.

16.1.6 Neurotransmitters and Receptors

Neurotransmitters are chemical signaling molecules released into the synaptic cleft from the presynaptic nerve terminal. The three major criteria that define a substance as a neurotransmitter are

1. The transmitter must be present within the presynaptic neuron.
2. The substance must be released in response to presynaptic depolarization, which must occur in a Ca^{2+}-dependent manner.
3. Specific receptors for the substance must be present on the postsynaptic cell.

In contrast to neurotransmitters, certain hormones typically influence target cells far removed from the hormone-secreting cells. This "action at a distance" is achieved by the release of hormones into the blood stream. Certain molecules such as vasopressin, oxytocin, and some other peptides may act as neurotransmitters in the brain, but as hormones in a different part of the body.

In general, neurotransmitters can be classified into two broad categories: small molecule neurotransmitters and neuropeptides. The small molecule neurotransmitters (Fig. 16.4) can be subdivided into acetylcholine, the amino acids (glutamate, aspartate, GABA, glycine), and the biogenic amines (dopamine, norepinephrine, epinephrine, serotonin, histamine). Neuropeptides are relatively large molecules composed of 3–36 amino acids. The peptide neurotransmitters may contain any different combinations of polar, hydrophobic, acidic, or basic amino acids.

The small molecule neurotransmitters are synthesized in the presynaptic nerve terminals. The precursor molecules are taken up by the nerve terminals by specific transporters. Following enzyme mediated synthesis (Fig. 16.5), the free neurotransmitter molecules are loaded into synaptic vesicles by specific vesicular membrane transport proteins. Following release of neurotransmitters into the synaptic cleft, they may bind to specific neuroreceptors on the membrane of the postsynaptic neuron. The transmitters may also be enzymatically degraded quickly or transported back (reuptake) into the presynaptic neuron by specific reuptake transporters.

Neuroreceptors are protein molecules embedded in the plasma membrane of the postsynaptic neuron. These receptors act as on and off switches for the receptor function. Each receptor has a distinctly shaped part that selectively recognizes a particular chemical messenger. A neurotransmitter fits into this region in much the same way as a key fits into a lock. When the transmitter is in place, this alters the neuron's outer membrane potential (excitability) by opening or closing the ion channels and triggers a change, such as the contraction of a muscle or increased activity of an enzyme in the cell.

Two broadly different families of receptors are involved in neurotransmitter–receptor interaction. (a) The ligand-gated ion channels combine the receptor site and ion channel in to one molecular entity and, therefore, give rise to rapid postsynaptic changes in the membrane potential. (b) Metabotropic receptors on the other hand, regulate the activity of ion channels indirectly, via G-proteins and induce slower, long lasting electrical response. These receptors may activate intracellular effector enzymes that modulate the phosphorylation of target proteins and/or gene transcription.

For each neurotransmitter, there may be more than one structurally and pharmacologically distinct receptor subtype (Table 16.1) that can be expressed on the membrane of a postsynaptic neuron depending on its exact location in the specific area of the brain. For example, dopamine has five receptor subtypes, while serotonin has fourteen 5-HT receptor subtypes (Barnes

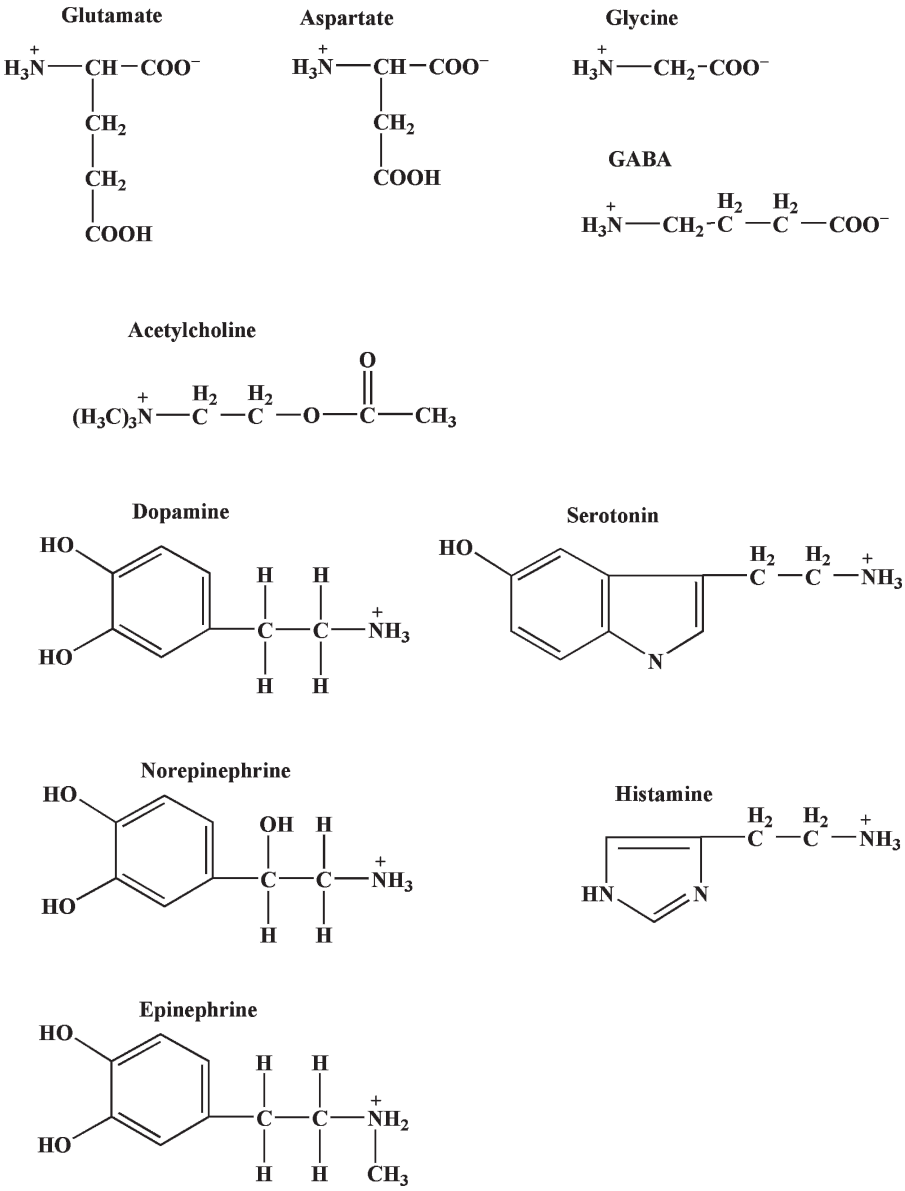

Fig. 16.4 The neurotransmitters can be chemically classified into three groups: amino acids, acetylcholine, and biogenic amines

and Sharp 1999). Following binding of a neurotransmitter to a specific receptor or receptor subtype, the postsynaptic response, at a given synapse, is, therefore, dictated by the combination of receptor subtypes, G-protein subtypes, and ion channels that are expressed in a particular postsynaptic neuron. The second messengers are molecules that trigger the biochemical communication within cells, after the action of neurotransmitters at their and these intracellular effects may be responsible for long-term changes in the nervous system. These messengers convey the chemical message of a neurotransmitter (the first messenger) from the cell membrane to the cell's internal biochemical machinery. The effects of the second messenger may last for a few milliseconds to many minutes.

Knowledge of the role neurotransmitters play in the brain and the effect of drugs on receptor molecules are two of the most frequently studied areas, in neuroscience. Armed with this information, scientists hope to understand the circuits responsible for disorders, such

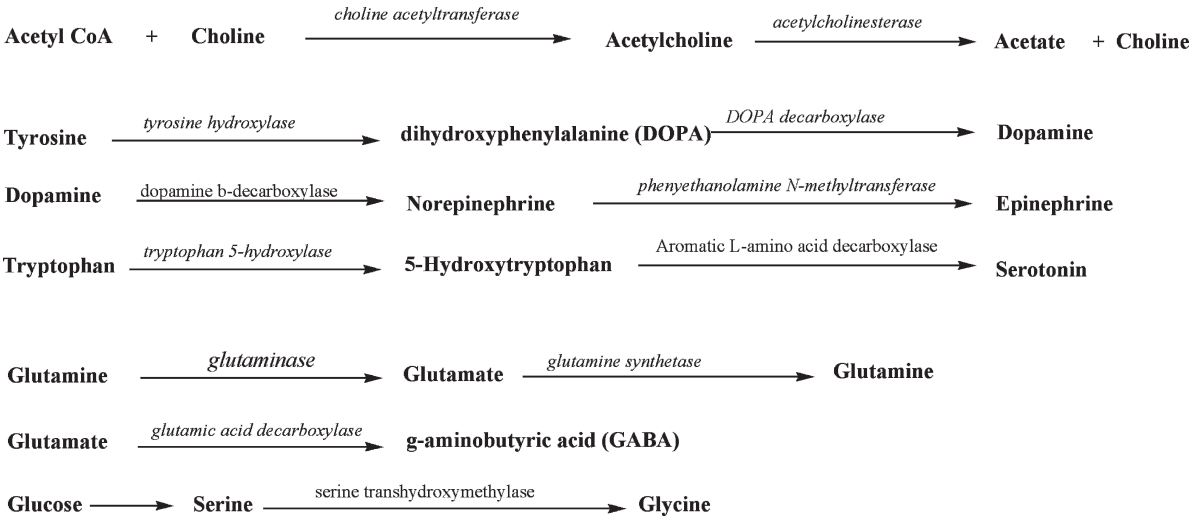

Fig. 16.5 The enzyme mediated synthesis of neurotransmitters in vivo

Table 16.1 Properties of some of the major neurotransmitters

Neurotransmitter	Receptors and subtypes	Postsynaptic effect	Specific role or functions
Acetylcholine (Ach)	Nicotinic, Muscuranic	Excitatory	Involved in muscle contraction, heart beat, memory, sleep, and normal attention
Glutamate	NMDA	Excitatory	Learning and memory
Aspartate	NMDA	Excitatory	
GABA	GABA	Inhibitory	Mood, Coordinate movement
Dopamine	D_1–D_5	Excitatory	Regulate movement, and endocrine function.
			Specific role in cognition and emotion.
Nor-epinephrine		Excitatory	Regulate heart rate and blood pressure, Learning and memory
Serotonin or 5-HT	5-HT_{1A}, 5-HT_{2A}	Excitatory	Sleep, mood, depression, anxiety
Enkephalin, Endorphin		Inhibitory	Minimize pain, induce sleep, enhance adaptive behavior

as Alzheimer's disease (AD), Parkinson's disease (PD), depression, and drug addiction. Sorting out the various chemical circuits involved in neuropsychiatric diseases is vital to understanding how the brain functions under normal physiological conditions and altered pathophysiological states. Radioisotope based molecular imaging probes provide the highest specificity and sensitivity needed to study and noninvasively image the neuroreceptor interaction within the human brain.

16.2 Radiopharmaceuticals for Functional Brain Imaging

The changes in electrical activity of neurons (excitation or inhibition) have been indirectly attributed to the alterations in the regional cerebral blood flow (rCBF) or local cerebral metabolic rate for glucose (LCMRglc). The functional coupling of rCBF and LCMRglc has

been well established in the normal human brain and certain neurological diseases. However, brain function is directly related to neural signaling and transmission of electrical activity via chemical and electrical synapses. In order to optimize the individualized patient treatment on the basis of targeted molecular therapies, and to select appropriate patients for specific drugs, need noninvasive molecular imaging techniques that can quantitatively assess the functional status and the underlying neurotransmitter and/or neuroreceptor abnormalities associated with a specific neuropsychiatric disease or disorder.

In general, there are four main classes of radiopharmaceuticals (Table 16.2) available for functional brain imaging studies to assess blood flow, metabolism, neurotransmission, and β-Amyloid plaques. A number of new, specific targeted molecular probes, designed specifically for both, diagnosis and assessment of treatment response, are under clinical evaluation. The potential clinical utility and limitations of the current, FDA approved radiopharmaceuticals and the new investigational drugs will be described briefly in this chapter.

16.2.1 Cerebral Blood Flow and Metabolism

CBF has been traditionally measured quantitatively either as a *flow rate*, expressed as volume of blood flowing per unit of time (mL min^{-1}) or as a *rate of tissue perfusion*, expressed as volume of blood flowing through a given quantity of tissue per unit of time (mL min^{-1} 100 g^{-1}). However, with respect to physiologic

Table 16.2 Radiopharmaceuticals for brain imaging studies

		Radiopharmaceutical	
Biological process	Target	PET	SPECT
Cerebral blood flow		[^{15}O]H_2O	^{99m}Tc-HMPAO (Ceretec™)
			^{99m}Tc-ECD (Neurolite™)
Glucose metabolism	*Hexokinase* and Glucose transporters	[^{18}F]FDG	
Neurotransmission	*AAAD*	[^{18}F]FDOPA	
	Dopamine	[^{11}C]SCH-23390	
	D_1 receptors	[^{11}C]NNC-112	
	Dopamine	[^{11}C]Raclopride	[^{123}I]IBZM
	D_2 receptors	[^{18}F]Fallypride	
	Dopamine transporters (DT)	[^{11}C]Cocaine	^{123}I-β-CIT
		[^{18}F]FP-CIT	^{123}I-Altropane
		[^{18}F]FE-CNT	^{99m}Tc-TRODAT1
	Vesicular amine transporter (VMAT)	[^{11}C]DTBZ	
		[^{18}F]DTBZ	
	5-HT_{1A} receptor	[^{11}C]DWAY	
		[^{18}F]MPPF	
	5-HT_{2A} receptor	[^{18}F]Altanserin	
		[^{18}F]Setoperone	
	5-HT transporter	[^{11}C](+)McN-5652	^{123}I-IDAM
		[^{11}C]DASP	
	mACh receptor	[^{18}F]FP-TZTP	
	nACh receptor	[^{18}F]NFEP	
		[^{11}C]PMP and AMP	
	μ-Opiate receptor	[^{11}C]Carfentanil	
	GABA receptor	[^{18}F]Flumazenil	^{123}I-Iomazenil
		[^{11}C]Flumazenil	
Amyloid plaques	β-Amyloid	[^{18}F]-FDDNP, [^{11}C]PIB	
		[^{18}F]-BAY94–9172	

function, perfusion directly relates to the supply of metabolic nutrient delivery to the tissue through the capillary beds. While there is a tight coupling between blood flow and metabolism in normal conditions, the coupling is disturbed in pathophysiologic conditions associated with several neuropsychiatric diseases.

A number of radiotracers have been used to assess CBF or perfusion. When the tracer reaches the capillaries, the process whereby a tracer leaves the blood pool and enters the tissue is critical for the quantitative measurement of perfusion. The fraction of the tracer which is extracted from the capillaries is referred to as the *extraction fraction* (*E*), a unitless parameter that can be estimated on the basis of the following Renkin-Crone equation:

$$E = 1 - e^{-PS/F} \tag{16.1}$$

The magnitude of *E* depends on the total available capillary surface area (*S*), the capillary permeability (*P*) for the tracer, and the blood flow (*F*). *E* increases as *S* or *P* increases, but decreases with increased *F*, because the tracer spends less time in the capillaries of that region. In the above equation, *P* for a specific radiopharmaceutical depends on the physicochemical properties of the radiotracer.

An ideal flow radiotracer accumulates in a tissue or clears from it, in proportion linear to the blood flow. Such a linear relationship between blood flow and uptake or clearance of the tracer should be constant and independent of pathophysiological changes and metabolism of that tissue. [^{15}O]water most closely meets the criteria of an ideal tracer for measuring blood flow or tissue perfusion. It is freely diffusible and the first-pass extraction approaches unity, and is independent of tissue blood flow and metabolic state. This tracer is, therefore, the most common radiotracer used for the measurement of rCBF (Raichle et al. 1983; Herscovitch et al. 1983). Besides [^{15}O]water, several other tracers such as [^{18}F]fluoromethane, [^{11}C]butanol, and ^{77}Kr have been used to image brain blood flow.

Since CBF is related primarily to the synaptic activity at the level of the neuron's cell body, the gray matter requires 3–4 times more blood flow compared to that of white matter. In the normal brain, the rCBF is dependent on vascular integrity, cerebral anatomy, and cerebral function. Over the years, the rCBF measurements, in normal human subjects, have provided quantitative estimation, but have yielded values that showed wide variation. Most published studies have reported values in the range of 40–80 mL min^{-1} 100 g^{-1} for gray matter structure, while a recent study has estimated the cortical global flow to be 62 ± 10 mL min^{-1} 100 g^{-1} (Meltzer et al. 2000).

SPECT radiopharmaceuticals for measuring rCBF are lipophilic agents, known as chemical microspheres, which are transported into the brain tissue by diffusion and subsequently trapped intracellularly, in proportion to the blood flow. Two of the agents used clinically are ^{99m}Tc-HMPAO (Ceretec®) and ^{99m}Tc-ECD (Neurolite®). While assessment of rCBF using SPECT tracers has provided diagnostic clinical information, the SPECT technique does not provide high resolution images and the data are not optimal for the quantitative estimation of rCBF and perfusion. In the future, dedicated neuro-SPECT scanners capable of attenuation and scatter correction may provide rCBF measurements that may be acceptable for evaluating the therapeutic response of drugs, designed to improve the CBF.

16.2.1.1 Cerebral Oxygen Metabolism

In addition, to the measurement of rCBF, estimation of the cerebral blood volume (CBV) and cerebral metabolic rate of oxygen ($CMRO_2$) permit the discrimination of various compensatory mechanisms in occlusive vascular diseases. The ratio of CBF/CBV indicates a perfusion reserve, while the oxygen extraction fraction (OEF) is a marker of a metabolic reserve. The OEF reflects arteriovenous oxygen difference divided by the arterial oxygen content. Almost 30–40 years ago, the methods of quantitative measurement of rCBF, $CMRO_2$ and OEF were described in detail (Ter-Pogossian et al. 1969; Jones et al. 1976; Frackowiak et al. 1980).

The continuous inhalation of either molecular oxygen, [^{15}O]O_2 or carbon dioxide, [^{15}O]CO_2, will generate complementary images relating regional oxygen uptake and blood flow, while the assessment of CBV can be performed using carbon monoxide, [^{15}O]CO, a tracer that would label RBCs in vivo. The $CMRO_2$ can be estimated on the basis of the following relationship (Frackowiak et al. 1980):

$$CMRO_2 = CBF \times OEF \times \text{total blood oxygen count} \tag{16.2}$$

CBF, $CMRO_2$, and OEF have been determined in normal human subjects (Table 16.3) on the basis of steady-state inhalation methods (Frackowiak et al. 1980).

Table 16.3 Normal Values

	CBF	$CMRO_2$		CMRglc	
Brain Region	mL/min/100 g	mL O_2/min/100 g	μmoles/min/100 g	mg/min/100 g	μmoles/min/100 g
Gray matter, temporal lobe	65.3 ± 7.0	5.88 ± 0.57	255 ± 25	7.9 ± 2.1	44 ± 12
Thalamus	–	–	–	6.5 ± 1.2	36 ± 7
White matter	21.4 ± 1.9	1.81 ± 0.22	78 ± 9	4.1 ± 1.4	23 ± 8

Data from Mazziotta et al. (1981)

Methods have also been developed to measure these quantitative parameters on the basis of the autoradiographic technique, using intravenous administration of $[^{15}O]H_2O$ (Herscovitch et al. 1983).

16.2.1.2 Cerebral Glucose Metabolism

The energy metabolism in the adult human brain depends almost completely on the oxidation of glucose (Siesjo 1978). Since the brain does not store these nutrients (oxygen and glucose), it has been hypothesized that rCBF is continuously regulated to supply these nutrients locally depending on the demands of neural activity.

FDG was initially developed as a tracer to assess cerebral glucose metabolism with PET (Phelps et al. 1979; Reivich et al. 1979). On the basis of arterial sampling of ^{18}F, blood activity, and dynamic FDG-PET imaging studies, the global and regional cerebral metabolic rates of glucose utilization (CMRglc) were estimated to be $100\,g^{-1}$ or μmoles min^{-1} $100\,g^{-1}$, by several investigators. The results from the UCLA group (Mazziotta et al. 1981) are listed in Table 16.3. Since serial blood sampling in the clinic is not practical, the brain FDG-PET scans are typically interpreted qualitatively with visual analysis of the relative distribution of the FDG regional uptake in a specific patient, compared to that in age-matched normal control subjects. Also, in addition to age, other factors, such as blood glucose levels, sex, handedness, sensory environment, level of alertness, mood, and drugs, may also influence the uptake of FDG in different areas of brain.

16.2.2 Neuroreceptor Imaging

The design, synthesis, and development of molecular neuroimaging radiopharmaceuticals for the assessment of neurotransmission are some of the most active areas of molecular imaging research. The estimation of the neuroreceptor occupancy is one of the most powerful examples of the utility of molecular imaging for developing CNS drugs for clinical trials and personalized patient therapy. The potential value of neuroreceptor imaging based on PET was first demonstrated in 1983, using the dopamine D_2 receptor ligand, $[^{11}C]$*N*-methylspiperone (Wagner et al. 1983). Since then, a number of PET and SPECT radiotracers have been developed to image neurotransmitter synthesis, neuroreceptor binding on the postsynaptic neuron, and specific transporters on the presynaptic neuron. Several review articles have discussed the development of receptor binding radiopharmaceuticals and their potential clinical applications (Fowler et al. 2003; Shiue and Welch 2004; Heiss and Herholz 2006; Hammoud et al. 2007). Some of the most promising agents shown to have potential clinical utility in several neuropsychiatric diseases are discussed below.

16.2.2.1 Dopamine System

Dopamine is synthesized in the dopaminergic neurons in the substantia nigra, the ventral tegmental area. and the retrorubral area of mesencephalon. Dopamine does not cross the BBB. It is synthesized in the neuron from the amino acid tyrosine and stored in the intracellular vesicles (Fig. 16.6). Specific vesicular amine transporters ($VMAT_2$) transport dopamine and other monoamines from the cytosol into the vesicles. The free dopamine in the cytosol is oxidized by the enzyme monoamine oxidase (MAO). Following release of the dopamine into the synapse, the dopamine interacts with the postsynaptic dopamine receptor sites. The five major subtypes of dopamine receptors can be classified into two major categories, depending on their ability to stimulate (D_1, D_5) or inhibit (D_2, D_3, D_4) adenylate cyclase, following binding to the receptor. The synaptic concentration of dopamine is regulated by the reuptake of dopamine into the presynaptic nerve terminal

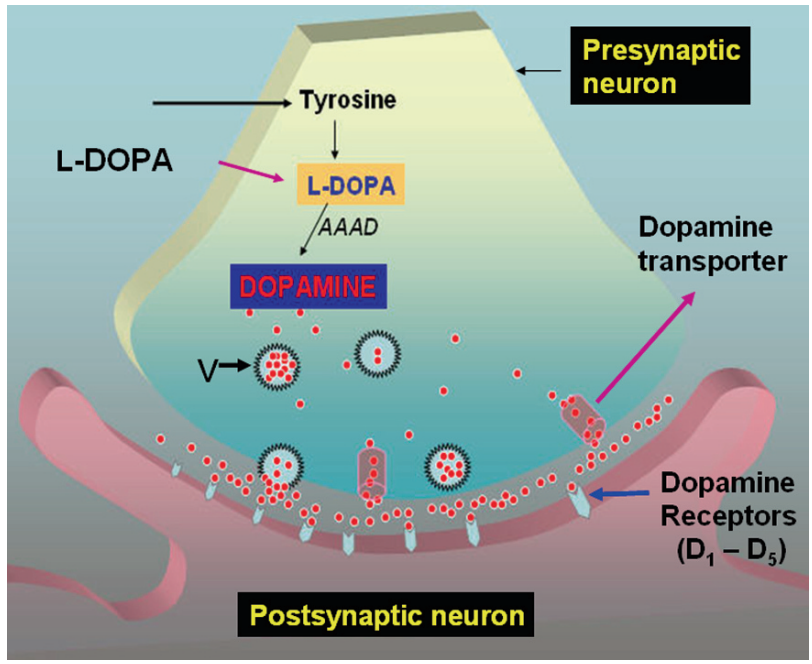

Fig. 16.6 The dopaminergic system: Dopamine, synthesized in the presynaptic neuron is stored in the vesicles (V) and released into the synapse. Dopamine binds to specific receptors on the postsynaptic membrane or is transported back into the presynaptic neuron via dopamine transporters

by specific dopamine transporters on the presynaptic plasma membrane. In the last three decades, the dopamine system has been a major focus in the development of PET and SPECT tracers.

Dopamine Metabolism

Since L-DOPA is the precursor for dopamine synthesis, [^{18}F]fluoro-L-DOPA (FDOPA) has been synthesized in order to image the dopamine synthesis and metabolism in the presynaptic nerve terminals (Garnett et al. 1983). FDOPA (Fig 16.7) is a substrate for the enzyme *AAAD, which* converts FDOPA to [^{18}F]fluorodopamine (FDA). Since tyrosine is the amino acid precursor for the synthesis of dopamine, both ^{18}F and ^{123}I- labeled *m*-tyrosine analogs have also been prepared (Fowler et al. 2003) and evaluated.

Dopamine Transporters

Following the synthesis of dopamine in the nerve terminal, the vesicular amine transporter (VMAT) transports the dopamine into the vesicles for storage. A more stable, stereoselective tracer, α(+)- [^{11}C]dihydrotetrabenazine (DTBZ) has also been developed (Frey et al. 1996). Further, [^{18}F]9-fluoropropyl-DTBZ (AV-133) was recently developed and evaluated in patients with PD.

Following the release of dopamine into the synapse, the dopamine is transported back into the presynaptic nerve terminal by a specific dopamine transporter (DAT) present on the presynaptic plasma membrane. The cocaine analog [^{11}C]cocaine (Fowler et al. 1987b) binds to this receptor, blocks the reuptake of dopamine, and increases the intrasynaptic dopamine levels. Therefore, a number of radiolabeled (^{11}C, ^{18}F, ^{123}I) analogs of cocaine have been prepared. Among them, [^{18}F] FP-CIT (Chaly et al. 1996), [^{18}F]FECNT (Zoghbi et al. 2006), and ^{123}I-altropane (Fischman et al. 2001) have shown clinical utility. On the basis of a N_2S_2 chelating agent, known as bisaminoethanethiol (BAT), the tropane analog, ^{99m}Tc-TRODAT-1, was developed for SPECT imaging studies (Kung et al. 2003). Several PET and SPECT tropane analogs, useful for imaging DATs, are shown in Fig. 16.8.

Dopamine Receptors

Among the dopamine receptor subtypes, D_1 and D_2 are highly concentrated in the striatum and a number of radiotracers have been investigated on the basis of dopamine D_2 receptor blocking antagonists (Fowler et al 2003). Initial studies were performed with ^{11}C and ^{18}F

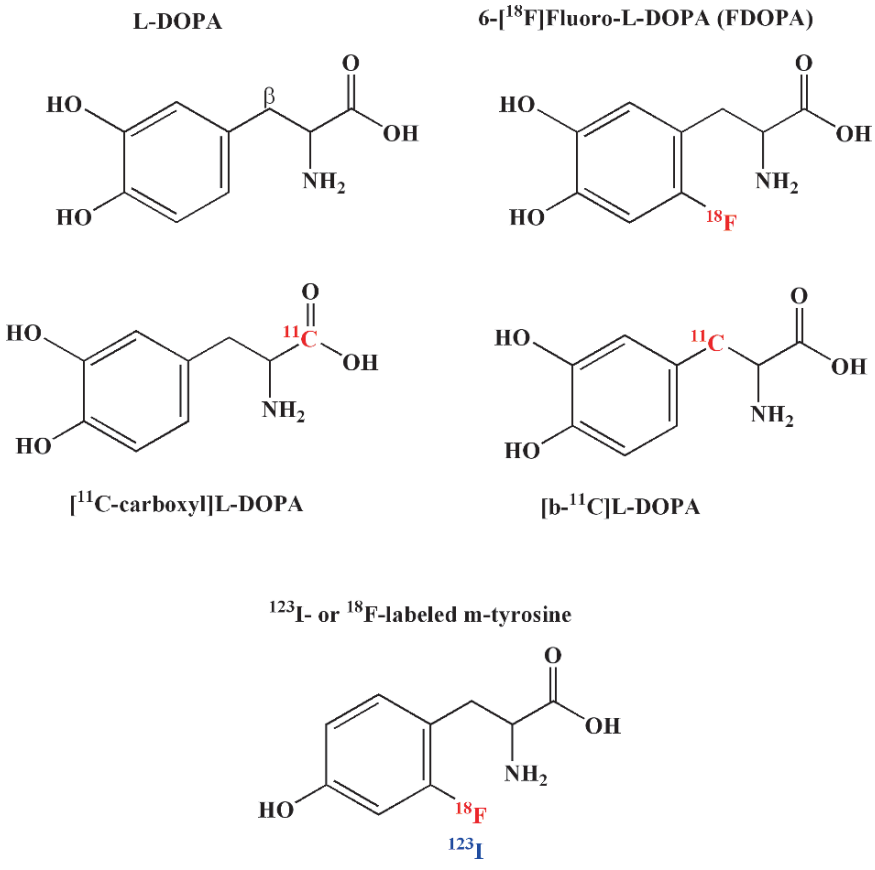

Fig. 16.7 Radiotracers used to image dopamine synthesis and metabolism in vivo

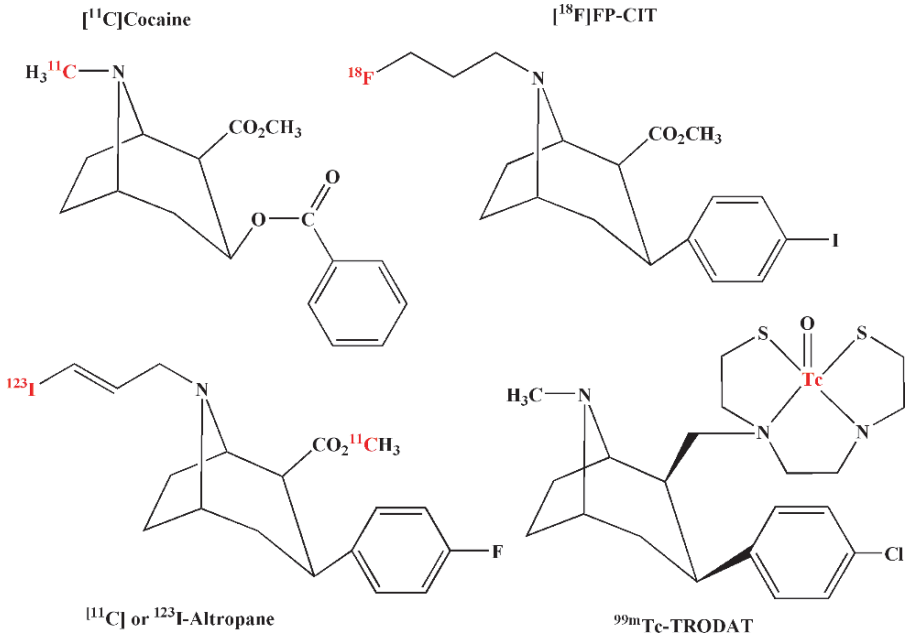

Fig. 16.8 PET and SPECT radioligands for dopamine transporter (DT)

labeled *N*-methylspiperidol (MSP), an irreversible antagonist that is not ideal for pharmacokinetic modeling and receptor quantitation studies. The benzamide analog, [^{11}C]raclopride, which has moderate affinity and reversible binding, is the most widely used PET tracer for imaging dopamine D_2 receptors, in vivo (Farde et al. 1985; Volkow et al. 1996). Radiotracer for SPECT,^{123}I-iodobenzamide (IBZM), has also shown to be very useful for assessing dopamine receptor density in human subjects (Kung et al. 2003a; Vallabhajosula et al. 1997). Among the high-affinity reversibly binding radiotracers, [^{18}F]fallypride (Mukherjee et al. 1999) provides a longer scanning period, while [^{11}C]FLB-457 (Halldin et al. 1995) has shown clinical utility to assess extrastriatal dopamine receptors.

Several tracers designed to image both, striatal and extrastriatal dopamine D_1 receptors has been evaluated. While [^{11}C]SCH-23390 is a well studied D_1 anatagonist, the positive enantiomer of [^{11}C]NNC-112 binds selectively and reversibly, and shows favorable pharmacokinetics for in vivo quantitation (Abi-Dargham et al. 2000) of D_1 receptors. Several radiotracers, useful for imaging dopamine D_2 and D_1 receptors, are shown in Figs. 16.9 and 16.10.

MAO Expression

The enzyme MAO oxidizes dopamine in the presynaptic neuron. The suicide enzyme inhibitors, clorgyline and deprenyl (Fig. 16.11) block the oxidation of dopamine and increase the dopamine levels in the nerve terminal. [^{11}C]clorgyline and [^{11}C]-L-deprenyl (deuterium-substituted derivative) have been used to image the expression of MAO-A and MAO-B in human subjects (Fowler et al. 1987a, 2003).

16.2.2.2 Serotonin System

The cells that produce serotonin in the brain are located in the dorsal raphae nucleus, which extensively innervates neocortical regions. The amino acid tryptophan is the precursor for the synthesis of serotonin in vivo. Tryptophan is first hydroxylated to form 5-Hydroxytryptophan (5-HTP). [^{11}C]5-HTP has been synthesized to assess serotonin metabolism, however, this tracer found its application in the imaging of neuroendocrine tumors. Another tracer, [^{11}C]α-methyl-L-tryptophan has been synthesized to monitor the serotonin synthesis, indirectly (Diksic et al. 2000). The enzyme *tryptophan hydroxylase* converts this precursor to [^{11}C]α-methylhydroxy-tryptophan which is then decarboxylated by *AAAD* to a more stable analog of serotonin, [^{11}C]α-methylserotonin, which may reflect the rate of the serotonin synthesis, in vivo.

Serotonin Receptors

Although 14 serotonin receptor subtypes are known (Barnes and Sharp 1999), the major emphasis in the

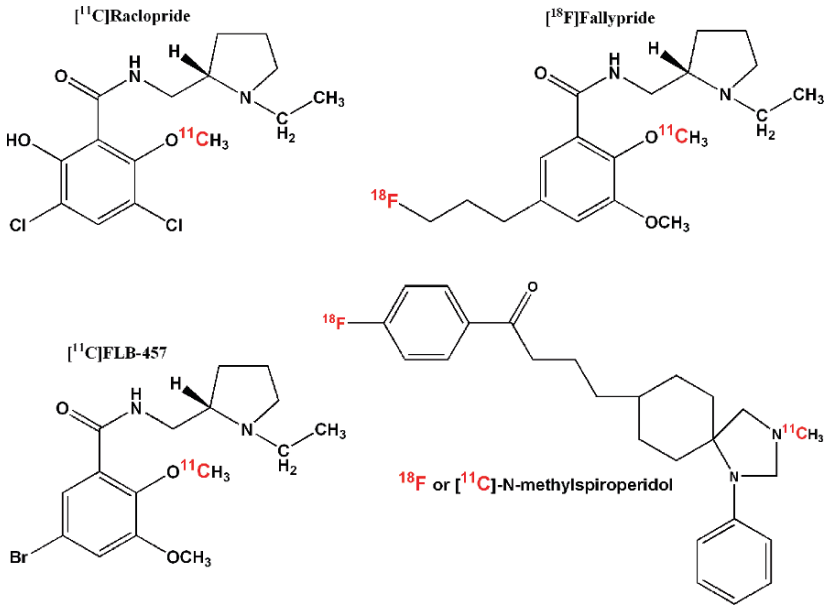

Fig. 16.9 PET radioligands for dopamine D_2 receptors

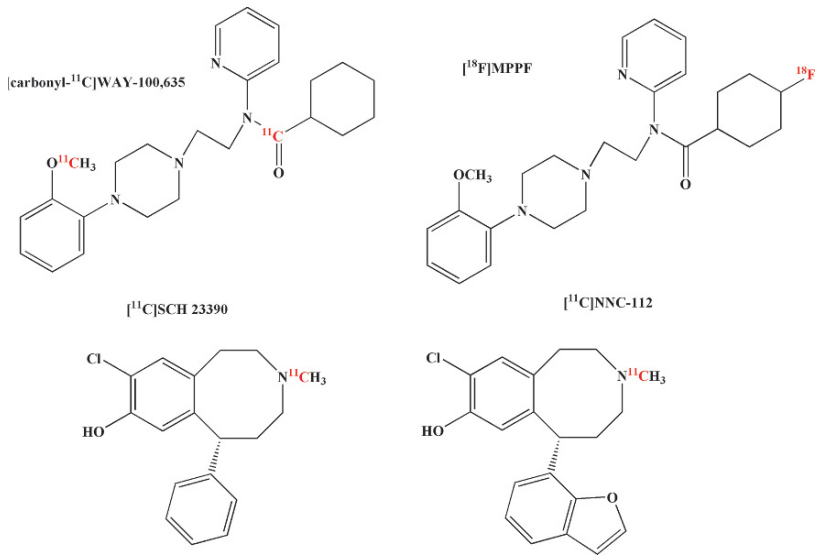

Fig. 16.10 PET radioligands for dopamine D_1 receptors

Fig. 16.11 Radioligands for the enzyme *monoamine oxidase (MAO)*

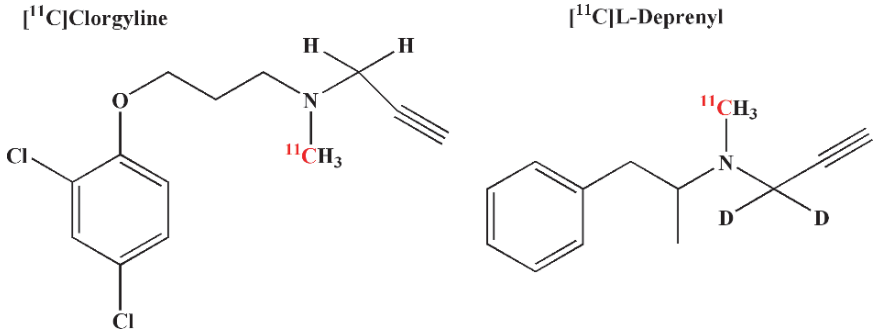

development of radiotracers has focused on the 5-HT_{1A} and 5-HT_{2A} receptor subtypes. The 5-HT_{1A} receptors are present on the cell bodies of raphe nuclei and serve as autoreceptors mediating serotonin release. Also, they are present at the pre- and postsynaptic serotonergic terminals. The highest densities of these receptors are located in the limbic forebrain (hippocampus, entorhinal cortex, and septum), while the lowest densities are found in the extrapyramidal areas (basal ganglia, substantia nigra) and in the cerebellum. The presynaptic sites have been proposed to mediate drug treatment of anxiety and depression, while the postsynaptic sites have been found to be elevated in schizophrenic brains postmortems (Fowler et al. 2003). The 5-HT_{2A} receptors are present in all neocartical regions, with a lower density in the hippocampus, basal ganglia, and thalamus, cerebellum and the structures of the brain stem are virtually devoid of these receptors (Herholz et al. 2004).

Some of the most important serotonin receptor binding radiotracers for PET imaging studies are shown in Figs. 16.12 and 16.13). Among the receptor antagonists, [O-methyl-^{11}C]WAY 100635 was the first radioligand used to image the 5-HT_{1A} receptors in humans. However, because of the formation of a more lipophilic metabolite in vivo with greater brain uptake, the tracer was found not to be optimal for imaging studies. However, the [carbonyl-^{11}C]desmethyl-WAY-100635 (DWAY) analogue, in which ^{11}C is labeled in a different position to prevent in vivo metabolism, has shown superior binding to the 5-HT_{1A} receptors (Passchier and van Waarde 2001). Because of their high affinities to this receptor subtype,

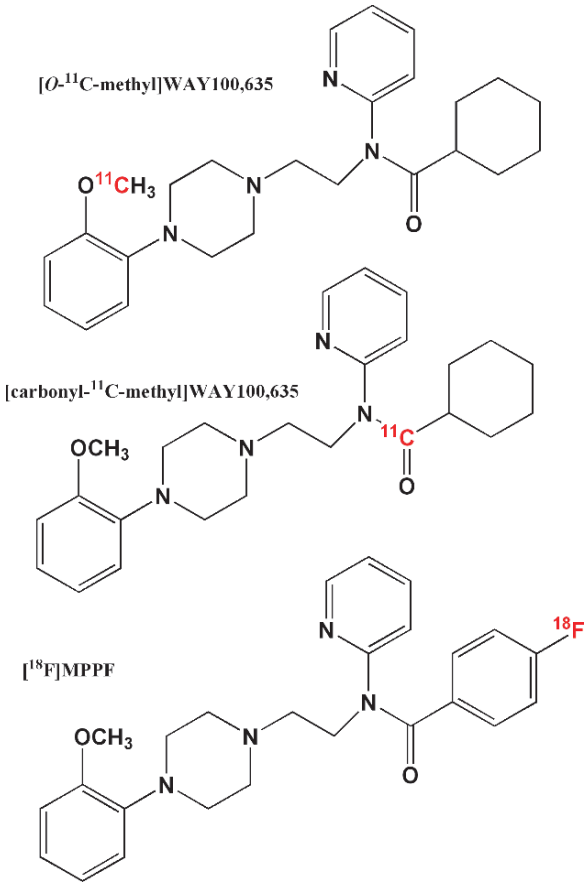

Fig. 16.12 PET radioligands for serotonin (5-HT_{1A}) receptors

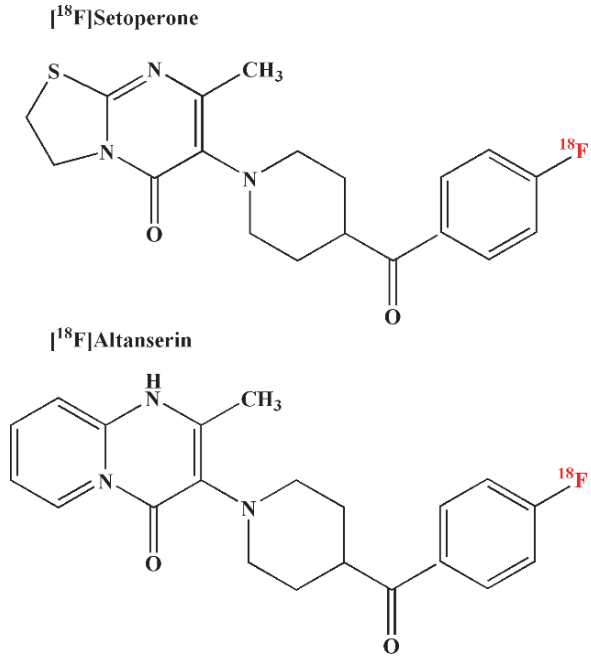

Fig. 16.13 PET radioligands for serotonin (5-HT_{2A}) receptors

both WAY and DWAY, however, may not be appropriate for measuring changes in the endogenous serotonin levels. In contrast, ^{18}F analogs of WAY100,635 have been developed to increase clinical applicability. [^{18}F]MPPF is selective for 5-HT_{1A} receptors and has been used to image 5-HT_{1A} receptors in the human brain, and its binding has been shown to be sensitive to endogenous serotonin (Passchier et al. 2000).

^{11}C or ^{18}F labeled NMSP, an irreversible antagonist used for imaging dopamine D_2 receptors in the basal ganglia, also bind to the 5-HT_{2A} receptors in the frontal cortex (Pike 1995). Among the more selective antagonists, [^{18}F]Altanserin provides slightly higher sensitivity for the detection of 5-HT_{2A} receptors and is one of the most selective antagonists utilized for imaging studies. Further, [^{18}F]Setoperone and [^{11}C]MDL 100,907 have also shown utility in imaging 5-HT_{2A} receptors in human studies.

Serotonin Transporter

Serotonin transporters (SERTs) belong to the same family as the other monoamine transporters, for the presynaptic reuptake of dopamine and norepinephrine. A number of antidepressent drugs (citalopram, fluoxetine, fluvoxamine, paroxetine, and sertraline) belong to the pharmacologic class of serotonin transporter reuptake inhibitors (Belmaker and Agam 2008). Because of the need to understand the mechanism of this disease and to evaluate the relative clinical efficacy of therapeutic agents, a number of molecular imaging radiotracers for PET and SPECT have been developed (Shieu and Welch 2004; Kung et al. 2003a; Heiss and Herholz 2006). [^{11}C](+)McN-5652 was the first successful radiotracer (Fig. 16.14) to show the expected regional brain distribution and uptake in the areas of higher receptor density (striatum, thalamus and midbrain). However, because of the in vivo metabolism, nonspecific binding, and poor signal contrast, this radiotracer is not ideal. A new class of potent SERT reuptake inhibitors, based on the parent compound phenylthiophenyl derivative known as 403U76 (Fig. 16.14), have been reported to possess high selectivity and affinity for SERT over norepinephrine and dopamine

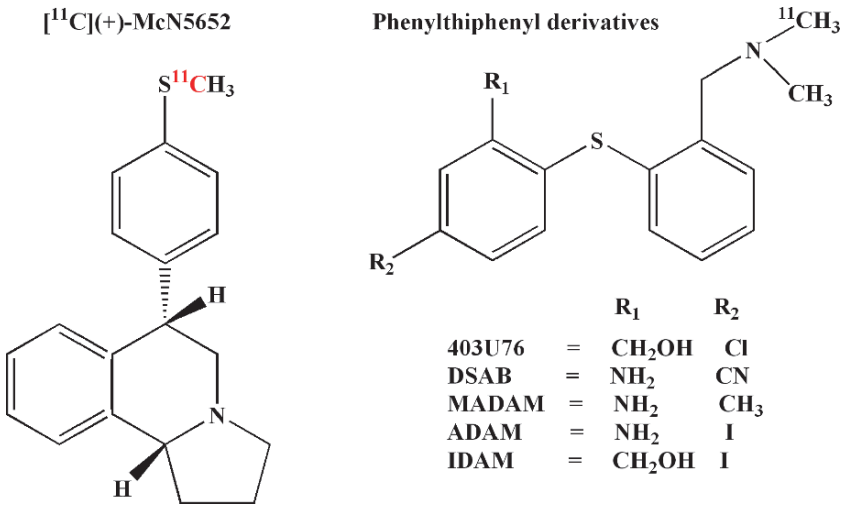

Fig. 16.14 PET and SPECT radioligands for serotonin transporters (ST)

transporter binding sites. Among the many PET tracers, [^{11}C]DASB, [^{11}C]DASP and [^{11}C]MADAM exhibit high affinity and selectivity for SERT and have proven to be excellent PET tracers for imaging SERT in the human brain (Ginovart et al. 2003; Heiss and Herholz 2006). On the basis of the 403U76 compound, ^{123}I labeled IDAM and ADAM were also prepared for SPECT imaging studies. Initial human studies have shown that [^{123}I]ADAM localizes in the hypothalamus, a region known to have SERT concentration and was found to be superior to [^{123}I]IDAM as a SPECT imaging agent for SERT in the brain (Kauppinen et al. 2003). Also, the cocaine analogs, ^{123}I-β-CIT and ^{123}I-nor-β-CIT, useful to image dopamine transporters, have shown uptake in SERT sites in patients with depression and schizophrenia (Kung et al. 2003a).

16.2.2.3 Cholinergic System

The neurotransmitter Ach plays a major role in learning, memory, and AD. Consequently, the receptors that mediate cholinergic neurotransmission and the enzymes that mediate its synthesis, as well as termination of its action, are the targets for developing specific radiotracers for imaging studies. Two types of receptors for Ach are known: the muscarinic-cholinergic receptors (mAChR) and the nicotinic-cholinergic receptors (nAChR), however, multiple heterogeneous subtypes have been characterized. While nAChRs belong to the ligand-gated ion channels, mAChrs operate via several second messengers.

Muscarinic Receptor

In the brain, mAChRs are the dominant postsynaptic cholinergic receptors. The first ligand to map mAChRs in humans was ^{123}I-QNB, 3-R-quinuclidinyl-4-S-iodobenzilate (RSIQNB) (Eckelman et al. 1984). Subsequently, several PET and SPECT tracers have been developed on the basis of receptor antagonists (Fig. 16.15), since they may have higher affinity and provide more image contrast. Most of these tracers, however, have very low receptor subtype selectivity and unfavorable receptor binding kinetics. Since radiotracers, based on receptor agonists, are more sensitive to the affinity state of the receptor and provide more biologically relevant information, an mAChR M_2 selective agonist, [^{18}F]FP-TZTP was developed (Eckelman 2001; Podruchny et al. 2003). Prior to the administration of physostigmine, an acetylcholinesterase (AChE) inhibitor, which would increase the intrasynaptic Ach levels, was found to produce a 35% reduction, thus, demonstrating specific binding of the radiotracer to mAChRs.

Nicotinic Receptor

The primary action site of nicotine are the nAChRs and these receptors are widely distributed in the CNS, PNS, and the adrenal glands. These receptors exist as pentamers comprised of α and β subunits, leading to considerable diversity. The most abundant subtype in the mammalian brain is $\alpha_4\beta_2$, which has the highest

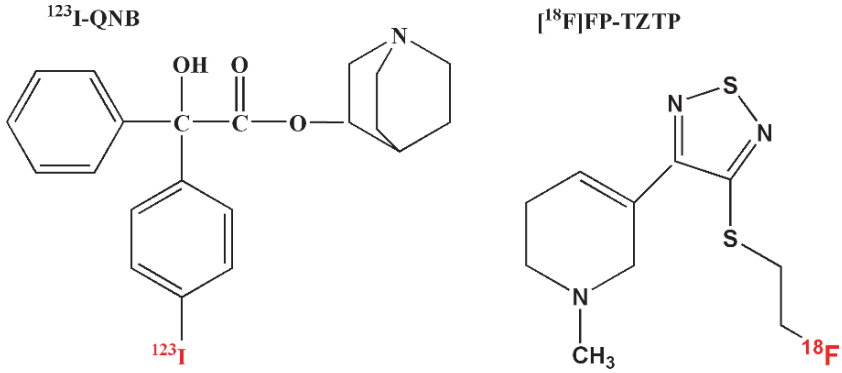

Fig. 16.15 PET radioligands for muscuranic cholinergic (mACh) receptors

affinity for nicotine (Fowler et al. 2003). [^{11}C]nicotine (Fig. 16.16) has been used in human studies and high binding was reported in several cortical and subcortical regions, while low density was found in the pons, cerebellum, occipital cortex, and white matter. Higher uptake was observed in smokers compared to non-smokers, indicating an increased density of nicotinic binding with the chronic administration of nicotine. However, the highly nonspecific binding and its rapid washout have limited the clinical application of this tracer. Other radiolabeled nicotinic agonists have also demonstrated suboptimal imaging characterisitics.

Epibatidine, a potent analgesic, isolated from the Ecuadorian poisonous frog, has a high specificity for nicotinic receptors. [^{18}F]norchloro-fluoroepibatidine (NFEP) has been used to image the nicotine receptor occupancy in animal models, however, it is not suitable for human studies because of unacceptable high toxicity (Ding et al. 2000). The most promising tracer for imaging nAChRs in humans is based on the 3-pyridyl ether derivatives of the parent compound A-85380, an agonist which has higher selectivity for $\alpha_4\beta_2$ receptor subtypes, but significantly lower toxicity.

Acetylcholinesterase

Since the enzyme AChE hydrolyzes Ach, it regulates the amount of Ach available in the synapse. AChE enzyme inhibitors, such as physostimine, increase the synaptic levels of ACh. As a result, [^{11}C]physostigmine (PHY) uptake and retention, in principle, represents the enzyme activity (Pappata et al. 1996). Labeled analogs of acetylcholine, which are also substrates for AChE, can be used to measure and image its activity in vivo (Fig. 16.16). These analogs are ^{11}C labeled *N*-methyl-4-piperidyl-acetate (MP4A, also known as AMP), which is 94% specific for AChE in the human brain, and *N*-methyl-4-piperidyl-propionate (MP4P or PMP). Hydrolysis of these tracers by AChE results in tissue trapping, while unhydrolysed tracers are washed out from the brain through blood flow (Koeppe et al. 1999; Herholz 2008).

16.2.2.4 Opiate System

Morphine and other opiate analgesic drugs, such as codeine, heroin and pethidine, affect the perception of pain by interacting with specific receptors expressed at a number of sites in the CNS and PNS. The endogenous opioids have been identified as a family of more than 20 peptides grouped into three classes: the endorphins, the enkephalins, and the dynorphins. Opiate receptors mediate the effects of opioid drugs and peptides in respiratory depression, analgesia, reward, and sedation. There are three opiate receptor subtypes; μ, δ, and κ. The μ subtype and its subclasses are the primary site for pleasurable reward feeling and the highest concentrations are found in the basal ganglia and thalamus. [^{11}C]Carfentanil (Fig. 16.17), a potent synthetic high affinity μ opiate receptor agonist was the first tracer investigated for opiate receptor imaging (Frost et al. 1985; Frost 2001). Its uptake in the basal ganglia and thalamus can be reduced by pretreatment with the opiate antagonist naloxone. Carfentanil binding is also sensitive to the release of endogenous opioids in response to pain. The high-affinity opiate antagonist [^{18}F]cyclofoxy binds to both μ and κ receptor sites and is distributed similarly to the distribution of naloxone in the caudate, amygdala, thalamus, and brain stem (Kling et al. 2000; Frost 2001).

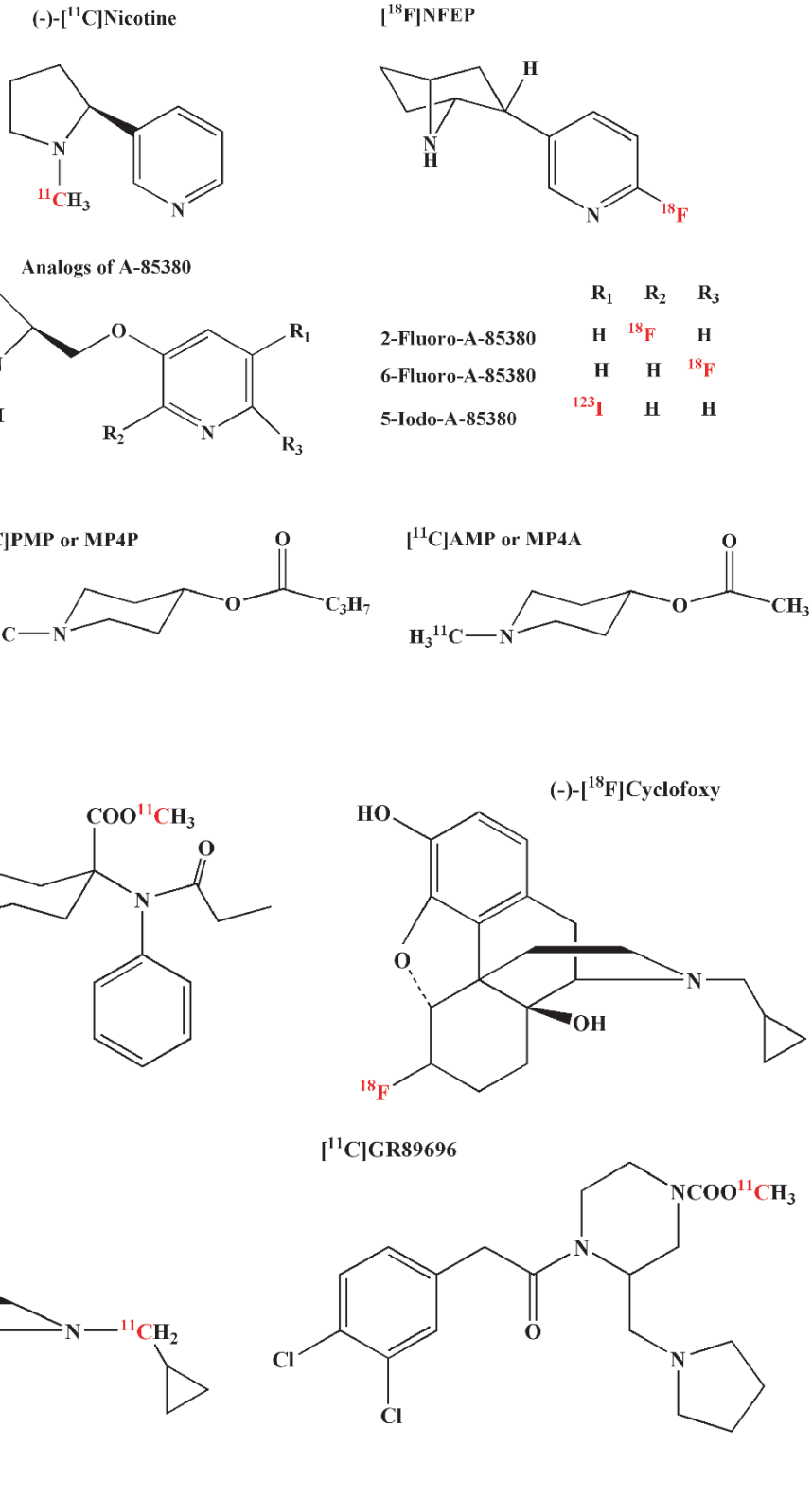

Fig. 16.16 PET radioligands for nicotinic cholinergic (nACh) receptors

Fig. 16.17 PET radioligands for opiate receptors

[^{11}C]Diprenorphine, a nonselective opioid agonist, and [^{11}C]buprenorphine, a compound with both agonist and antagonist properties, have also been developed for opiate receptor imaging studies. Diprenorphine clears more rapidly from the cerebellum, making it more appropriate for imaging studies, however, buprenorphine has low toxicity and is an approved analgesic drug. Recent studies have shown that [^{11}C] GR103545, a stereotactic isomer of a potent κ-opioid receptor agonist, GR89696, displays excellent brain penetration and uptake kinetics (Talbot et al. 2005).

16.2.2.5 GABA System

γ-Aminobutyric acid (GABA), the most important inhibitory neurotransmitter in the brain, interacts with the GABA receptor system which is abundant in the cortex. Part of the $GABA_A$ receptor complex, which gates the Cl_2 channel, is the central benzodiazepine receptor, which specifically mediates all pharmacologic properties of drugs, which are known as the benzodiazepines (sedative, anxiolytic, anticonvulsant, myorelaxant) (Heiss and Herholz 2006). Binding sites for these benzodiazepines have been subdivided into *central* and *peripheral* types. Only the central sites are associated with neuronal $GABA_A$ receptors, while the peripheral binding sites in the brain are only expressed by non-neuronal microglia and ependymal cells. The peripheral sites also occur in the kidneys, liver, lungs, mast cells, and macrophages.

The radiotracers most widely used for imaging central benzodiazepine-binding sites (Fig. 16.18) are based on the antagonist, Ro-15-1788 (flumazenil). With [^{11}C] flumazenil, a clear dose-dependent binding has been demonstrated (Persson et al. 1985). The ^{123}I labeled analog, iomezenil, developed for SPECT studies, has also been labeled with ^{11}C for use in PET studies (Bremmer et al. 2000). Finally, a high specific activity ^{18}F labeled flumazenil was also developed (Ryzhikov et al. 2005). These tracers bind mainly to a α_1 subtype of the $GABA_A$ receptors in the medial occipital cortex, followed by other cortical areas (the cerebellum, thalamus, striatum, and pons). [^{11}C]Ro-15-4513 (azidomazenil), a partial inverse agonist, which binds preferentially to the α_5 receptor subtype, has shown greater uptake in limbic areas, particularly in the anterior cingulate cortex, hippocampus, and insular cortex, but lower uptake in the occipital cortex and cerebellum compared to flumazenil (Suhara et al. 2003a).

The tracer most frequently used as the ligand for the peripheral benzodiazepine receptor (PBR) is the isoquinoline, [^{11}C]PK-11195 (Fig. 16.19), which binds to activated, but not resting, microglia (Banati et al. 2000).

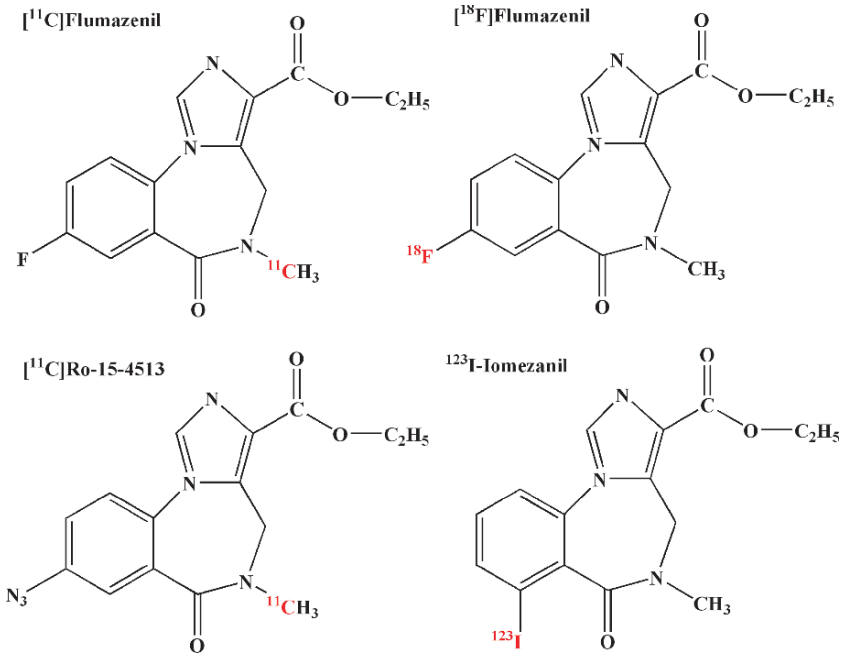

Fig. 16.18 PET and SPECT radioligands for GABA system (central benzodiazepine receptors)

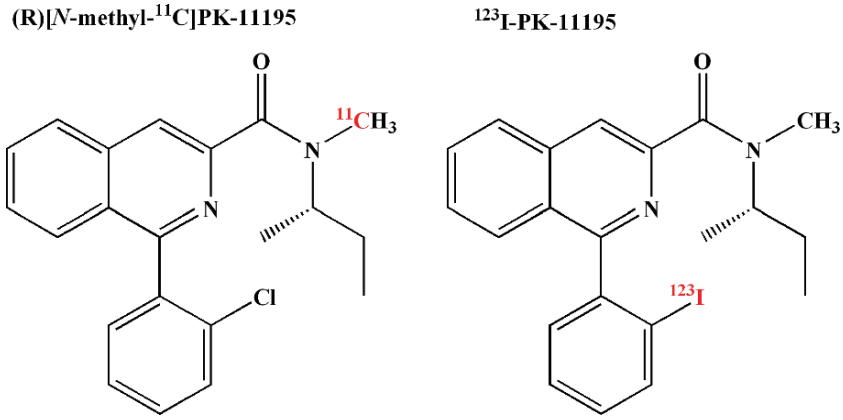

Fig. 16.19 PET and SPECT radioligands for peripheral benzo-diazepine receptors

This tracer has been used to image active brain pathology associated with microglial activation and neurodegenerative conditions, including stroke, multiple sclerosis, encephalitis, PD, and AD. While PK11195 has provided the proof-of-principle that the estimation of PBR expression in vivo is possible, the high degree of nonspecific uptake of PK11195 complicates the quantification and modeling of the PET data. Other ligands displaying better brain kinetics have recently been described. Among them, [^{11}C]DPA-713, a compound from the family of pyrazolopyrimidines, has shown a higher affinity for PBR than PK11195. Also, [^{11}C]DPA-713 is substantially more selective for the PBR than for the CBR (Thominiaux et al. 2006, Boutin et al 2007).

16.2.3 β-Amyloid Imaging

Neuropathologic evidence suggests that the characteristic neuropathologic hallmark in AD is the deposition of senile plaques (SPs) which contain β-amyloid (Aβ) aggregates and neurofibrillary tangles (NFTs) consisting of highly phosphorylated tau protein (Morris and Naggy 2004). The main constituents of Aβ-deposits in the AD brain are peptides of 40 and 42 amino acids, $A\beta_{40}$ and $A\beta_{42}$, respectively, generated from the cleavage of the amyloid precursor protein (Fig. 16.20) (Price 1997). The subsequent arrangement of these peptide monomers into an amyloid fibril results in a characteristic β-plated sheet structure, which represents the target for tracers developed for noninvasive molecular imaging probes.

Compact plaques consist of a dense central core of amyloid fibrils, while noncompact plaques contain less fibrillar Aβ (Dickson 1997). A shift of the brain Aβ from the soluble to the fibrillar form is closely associated with the onset of AD (Wang et al. 1999). Previous neuropathologic studies have indicated that neuritic plaque densities are highest in the neocortex, especially in the temporoparieto– occipital region, and lowest in the cerebellum.

16.2.3.1 Radiotracers for Imaging Aβ Aggregates

The four promising chemical backbones for amyloid radioligands include aminonapthalenes, benzothiazoles, stilbenes, and imidazopyridines, from which several compounds have been developed as imaging probes to detect amyloid in the brain. The structures of three important tracers, [^{18}F]-FDDNP, [^{11}C]PIB, and [^{11}C]SB-13, are shown in Fig. 16.21.

The first radio tracer described was [^{18}F]-FDDNP which is based on aminonaphthalene (Bario et al. 1999). In vitro binding studies have shown that FDDNP is was bound to the synthetic Aβ1–40 with two binding sites, a high affinity site (0.12 nM) and a low-affinity site (1.9 nM). In contrast, [^{18}F]-FDDP binding studies with postmortem AD homogenates have shown a Bmax value of 144 nM with a K_D value of 0.75 nM (Agdeppa et al. 2001).

N-Methyl-[^{11}C]-2-(49-ethylaminophenyl)-6-hydroxy-benzothiazole or [^{11}C]-6-OH-BTA-1 (also known as Pittsburgh Compound-B or PIB) was developed on the basis of the thioflavin-T amyloid dye

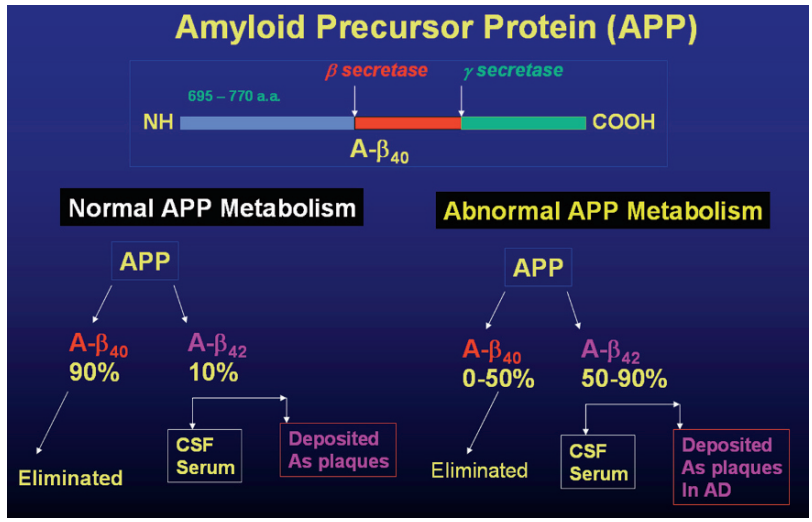

Fig. 16.20 Amyloid precursor protein (APP) metabolism, elimination, and deposition in brain

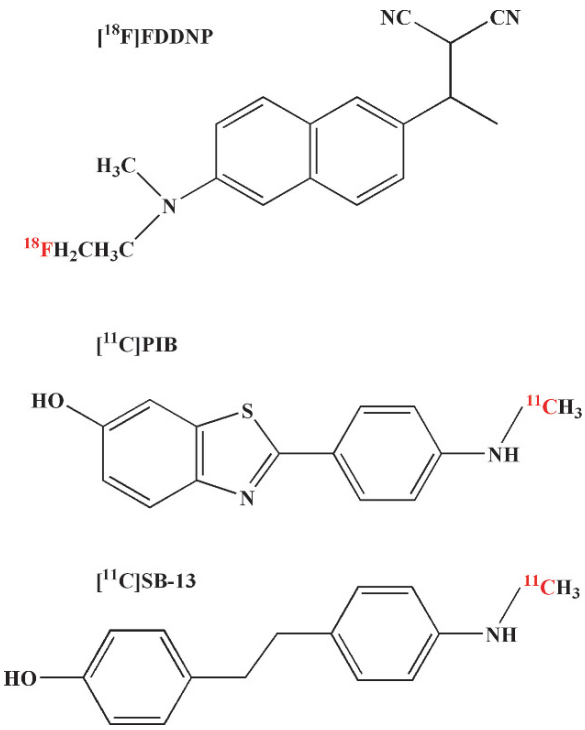

Fig. 16.21 PET radiotracers for imaging brain β-amyloid plaques and tangles in patients with Alzheimer's disease

(Mathis et al. 2002). PIB has shown two binding sites in human autopsy brain tissue, a high affinity binding site with a B_{max} of 1,407 pmol g^{-1} and a K_D value of 2.5 nM, and a low-affinity binding site with a B_{max} of 13 nM and a K_D of 250 nM, respectively. Avid Pharmaceuticals recently reported the development of an ^{18}F labeled stilbene derivative, ^{18}F-BAY94–9182 (also known as ^{18}F-AV1/ZK), which shares common structural features with PIB (Zhang et al. 2005a, b). This tracer has been shown to bind avidly to neuritic and diffuse Aβ plaques, and to cerebral amyloid angiopathy in vitro (it does not show appreciable labeling of tangles, Pick bodies, Lewy bodies, or glial cytoplasmic inclusions). In brain homogenates from patients with AD, BAY94–9172 (Fig. 16.22) was found to bind with high affinity (67 nM), and in AD tissue sections, it selectively labeled Aβ plaques (Thominiaux et al. 2006). On the basis of the SB-13 ligand, the ^{123}I labeled tracer, 6-iodo-2-(4V-dimethylamino-)phenyl-imidazo[1,2-a] pyridine (the ^{123}I-IMPY) was developed for SPECT imaging of brain amyloid depositions (Kung et al. 2003b).

16.3 Applications in Clinical Neurology

Clinical examination is more powerful in neurology than in many other medical specialties with respect to its ability to precisely localize a lesion in various neuropathological conditions. As a result, neurologists, traditionally, are less inclined to pursue imaging techniques to guide medical management. While abnormal neuropathology can be easily documented with morphological imaging techniques, such as CT and MRI, many aspects of neurologic diseases, in particular the molecular mechanisms that underlie their clinical

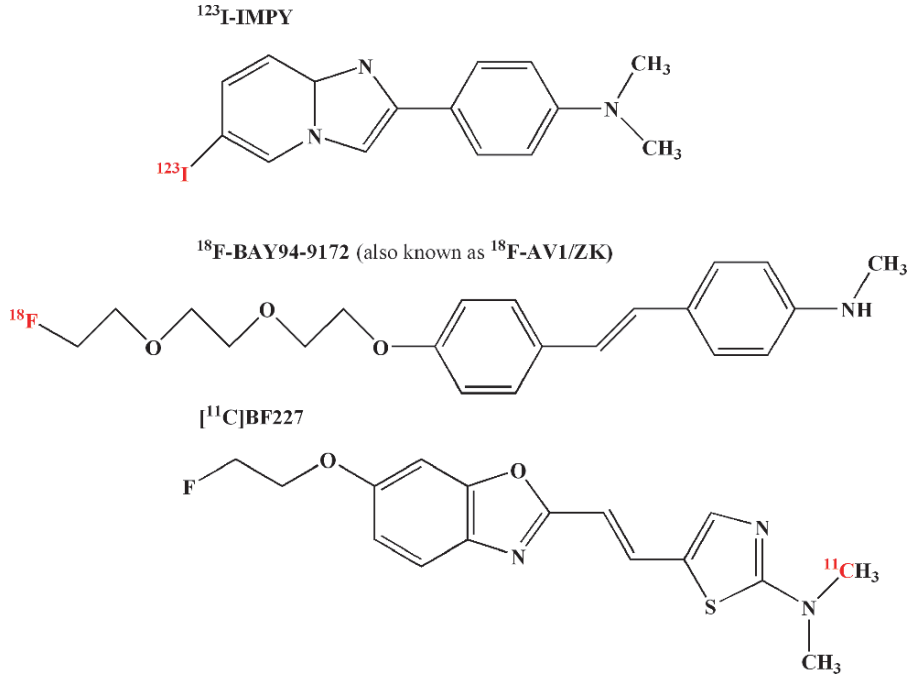

Fig. 16.22 PET and SPECT radiotracers for imaging brain β-amyloid plaques in patients with Alzheimer's disease

manifestation, cannot adequately be studied in vivo by clinical means and structural imaging (Herholz and Heiss 2004). In order to optimize individualized patient treatment, based on targeted molecular therapies, requires the selection of appropriate patients for specific drugs needs noninvasive molecular imaging techniques that can quantitatively assess the functional status, and the underlying neurotransmitter and/or neuroreceptor abnormalities associated with a specific neuropsychiatric disease or disorder. The changes in electrical activity of neurons (excitation or inhibition) have been indirectly attributed to the alterations in rCBF or LCMRglc. The functional coupling of rCBF and LCMRglc has been well established in the normal human brain and certain neurological diseases. With the availability of multimodality imaging technologies (such as PET/CT, SPECT/CT), radioisotope based molecular imaging radiopharmaceuticals will play a significant role in routine clinical management. The main areas in clinical neurology where molecular imaging techniques would play a major role are

- Diagnosis of AD and other dementias
- Differential diagnosis of movement disorders
- Localization of epileptic foci
- Diagnosis of primary and recurrent brain tumors
- Identification of viable tissue in ischemic stroke

In addition, molecular imaging will have great implications for the identification of potential molecular therapeutic targets, in the development of new treatment strategies, and in their successful implementation in clinical application. Various PET and SPECT radiopharmaceuticals with potential applications in clinical neurology are summarized in Table. 16.2. Some of the important clinical studies documenting the utility of these tracers are briefly described below.

16.3.1 Alzheimer's Disease

Dementia is a clinical syndrome characterized by impaired short- and long-term memory and is associated with deficits in abstract thinking, judgment, and other higher cortical functions. The degree of cognitive dysfunction, however, spans a wide spectrum. AD is a progressive, neurodegenerative disease characterized by loss of function and death of neurons in several brain areas, leading to the decline of prominent mental functions, including memory. AD is the most common cause of dementia in aging. AD was first characterized by Aloise Azheimer in 1907, who discovered that amyloid plaque (Aβ and NFTs) in the brain is a hallmark of this disease and the marker by which diagnosis is

confirmed, posthumously. One prominent hypothesis is that amyloid deposits and soluble forms of amyloid lead to neuronal dysfunction and cell death. The physiological role of Aβ is not exactly clear, but there is growing evidence which suggests that it is essential for the modulation of synaptic activity and neuronal survival under normal conditions (Drzezga 2008). Mild cognitive impairment (MCI) is considered a transitional stage between healthy aging (HA) and AD. Other causes of cognitive decline include dementia with Lewy bodies (DLB), vascular dementia (VD), frontotemporal dementia (FTD), Creutzfeldt–Jakob disease, HIV-associated dementia, neurosyphilis, Parkinson's dementia, normal pressure hydrocephalus, and dementias caused by exposure to toxic substances (heavy metals, alcohol, drugs), metabolic abnormalities, or psychiatric disorders (Herholz et al. 2004).

Although the exact causalities of most primary forms of dementias are not yet fully understood, growing evidence has been collected, supporting the assumptions that a common basis of many neurodegenerative dementias can be found in the increased production, misfolding, and pathological aggregation of proteins, such as β-amyloid, τ-protein, a-synuclein, or the recently described ubiquitinated TDP-43 (Drzezga 2008). In addition, amyloid pathology may occur in different stages of aggregation (oligomers, fibrils, plaques, etc.); it may show different configurations (diffuse, compact plaques, vascular amyloid, etc.) and different components ($A\beta_{40}$, $A\beta_{42}$, dystrophic neurites, etc.). The term Lewy bodies describes intracellular aggregations, mainly constituted of the a-synuclein protein, which is predominantly expressed in neurons.

Neuropathological studies indicate that two proteins, β-amyloid (in senile plaques) and τ-protein (in NFTs) accumulate abnormally in a predictable spatial pattern during aging and in AD (Mathis et al. 2007). Until recently, plaques and tangles could be assessed only during an autopsy or, rarely, during a biopsy.

The identification and differential diagnosis of AD is especially challenging in its early stages, such as MCI, partly because of the difficulty in distinguishing it from the mild decline in memory that can occur with normal aging and from mild cognitive manifestations of other neuropsychiatric conditions, such as depression, as well as other causes of dementia (Silverman et al. 2008). PET and SPECT have long been used to assess various forms of dementia, especially AD. The role of different molecular imaging probes with specific clinical applications are briefly summarized below.

16.3.1.1 FDG-PET in AD

AD is progressive and is commonly unrecognized in its very early stages. Since functional changes usually precede the anatomic changes seen on CT and MR images, FDG-PET has been investigated extensively in the evaluation of AD. Classically, patients with AD have a pattern of bilateral parietotemporal hypometabolism that is not generally seen in patients with other forms of dementia or in age matched control subjects (Silverman 2004) (Fig. 16.23). Further, asymmetry of the metabolic deficits is not uncommon. The decline of the FDG uptake in the posterior cingulate, hippocampus, parietotemporal, and prefrontal association cortices (Fig. 16.24) allows for the identification of mild to moderate AD with high sensitivity and specificity. Also, there is typically sparing of the basal ganglia, thalamus, cerebellum, and primary sensory cortex. Even early in the disease process, before the appearance of volume loss, FDG-PET has been helpful in diagnosing AD. Histopathologically confirmed sensitivity and specificity of PET for detecting the presence of AD are in the range of 92–94% and 71–73%, respectively (Silverman et al. 2008). Since medications used to treat AD continue to emerge and since these medications have demonstrated the ability to improve memory, or at least delay the deterioration of cognitive functions, (Herholz et al. 2004), FDG-PET imaging could aid in determining patient prognosis, disease progression, and the efficacy of various medication regimens.

16.3.1.2 β-Amyloid

Initial studies with [^{18}F]FDDNP have shown that PET scans show significantly higher values for FDDNP binding in the temporal, parietal, and frontal regions of the brain in patients with AD than in older control subjects without cognitive impairment (Shoghi-Jadid et al. 2002). More specifically, these studies have demonstrated a significantly greater "relative retention time" in AD subjects than control subjects, in the hippocampus, amygdala, and enthorhinal cortex, areas with high concentrations of plaques and tangles

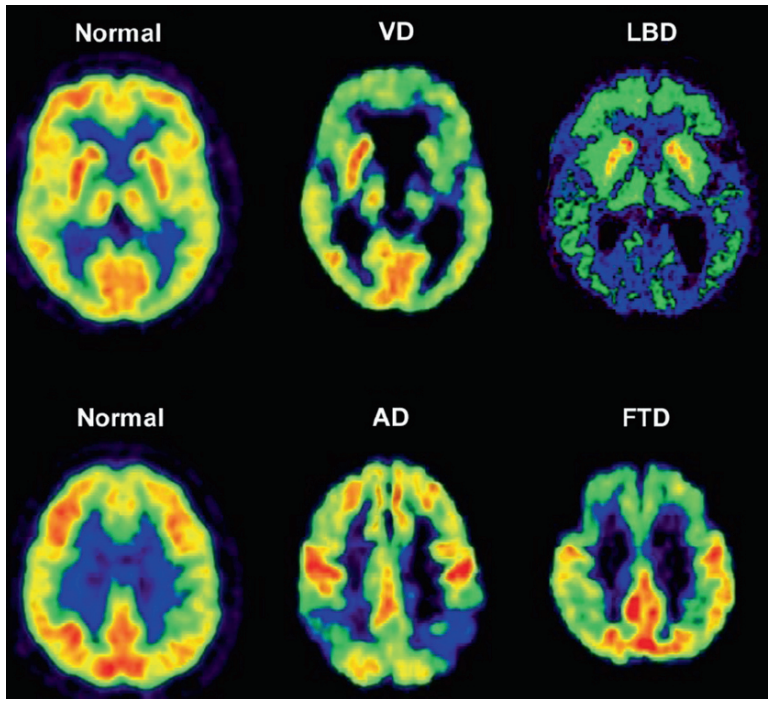

Fig. 16.23 FDG-PET showing hypometabolism in AD and differential diagnosis of AD from other forms of dementia (Jacobs et al. 2005)

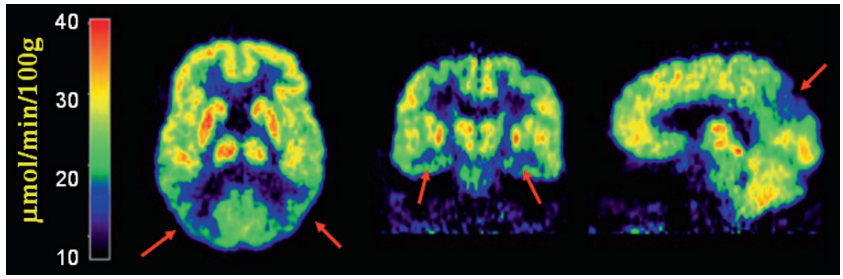

Fig. 16.24 FDG-PET in AD showing typical areas of hypometabolism in posterior cingulate, parietotemporal, and temporomesial cortices (Jacobs et al. 2005)

(Fig. 16.25). In a recent clinical study, FDDNP-PET scans appeared to differentiate persons with MCI from those with AD and those without cognitive impairment. Also, in vivo distributions of FDDNP in the brain followed patterns of pathological distribution seen during autopsy (Small et al. 2006). Limitations of this compound include high nonspecific binding (with a relatively low target-to-background ratio), low brain uptake (only about 9% higher cortical uptake), and lack of validated kinetic methods for quantitation (Shoghi-Jadid et al. 2002).

Studies with [^{11}C]PIB, the most specific and widely used radiotracer for Aβ, indicate that PIB-PET may allow earlier diagnosis of AD and accurate differential diagnosis of the dementias (Klunk et al. 2004; Mintun et al. 2006; Ng et al. 2007; Drzezga 2008). PIB-PET images (Fig. 16.26) show robust cortical binding in almost all AD patients (about 70% increase in cortical binding) and correlate well with a reduction in CSF $A\beta_{42}$. An inverse significant correlation has also been observed between brain PIB uptake in specific areas, and the corresponding glucose hypometabolism in the same areas imaged by FDG-PET (Klunk et al. 2004). In addition, PIB binding also correlates with the rate of cerebral atrophy as measured by MRI and with episodic memory impairment in apparently normal elderly individuals, and in patients with mild cognitive impairment (Archer et al. 2006). Increased PIB binding may also be predictive of the conversion of MCI to AD (Pike et al. 2007). Furthermore, the positive findings with PIB in AD subjects have been confirmed in more than 500 subjects by several research groups worldwide.

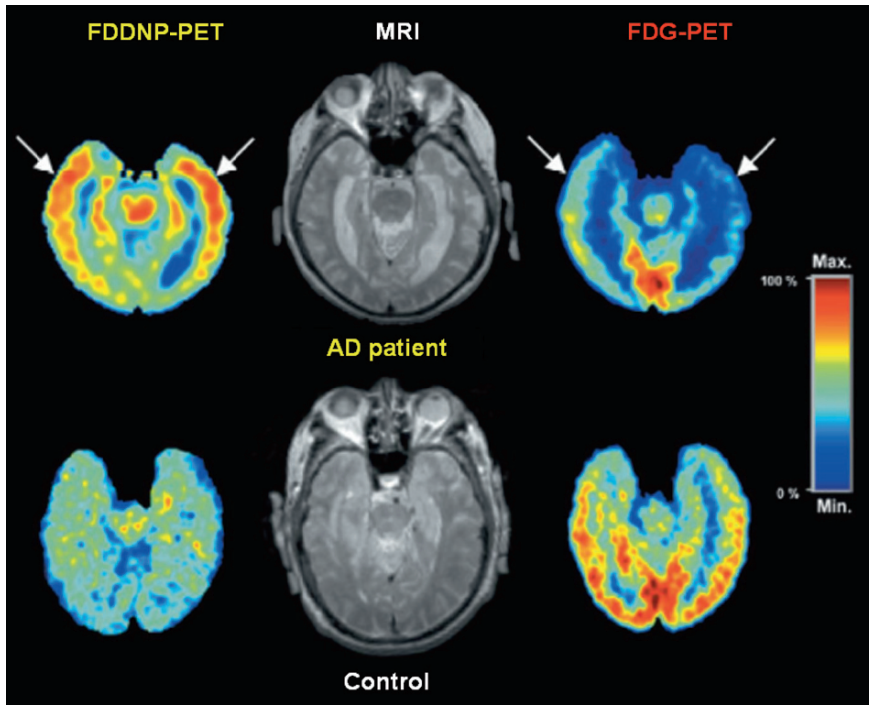

Fig. 16.25 Comparison of [^{18}F]FDDNP-PET and FDG-PET images in a patient with AD and a normal control subject. Brain areas with decreased FDG uptake show high retention and localization of FDDNP in a patient with AD, but not in normal subjects (Shoghi-Jadid et al. 2002)

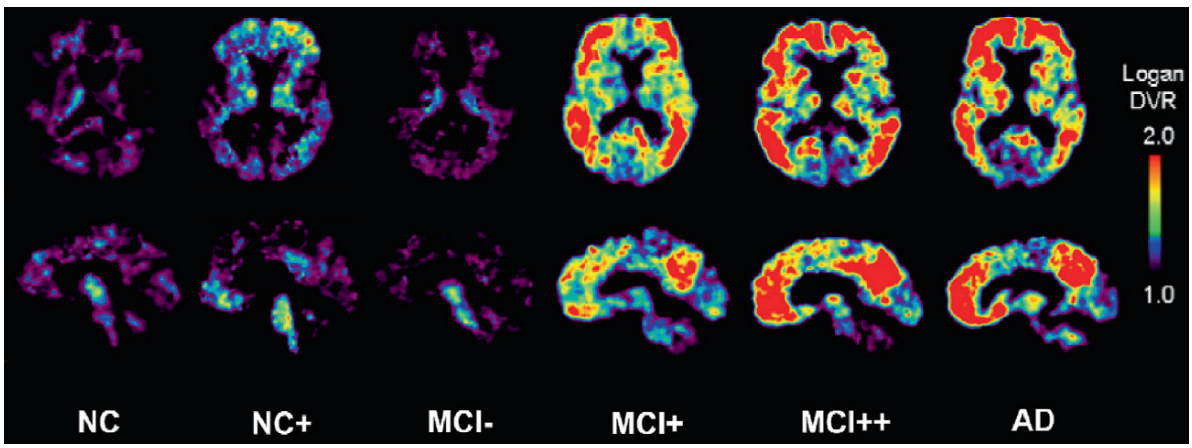

Fig. 16.26 [^{11}C]PIB-PET images (in the transaxial and sagittal planes) of parametric Logan distribution volume ratios (DVR) relative to the cerebellum in two normal controls (NC), three MCI subjects, and one AD subject. PIB uptake and retention may be either negative (–) or positive (+, ++) (Mathis et al. 2007)

In a recent clinical study, a stilbene derivative, ^{18}F-AV1/ZK, has demonstrated (Fig. 16.27) the potential value of Aβ-PET imaging to discriminate between AD patients and individuals with frontotemporal lobar degeneration (FTLD) or healthy controls and might facilitate integration of Aβ imaging into clinical practice (Rowe et al. 2008). AD patients have also shown widespread neocortical binding, which was greater in the precuneus/posterior cingulate and frontal cortex than in the lateral temporal and parietal cortex, and with relative sparing of the sensorimotor, occipital, and medial temporal cortex. Healthy controls and FTLD patients have also shown only white-matter binding, although three controls and one FTLD patient had mild uptake in the

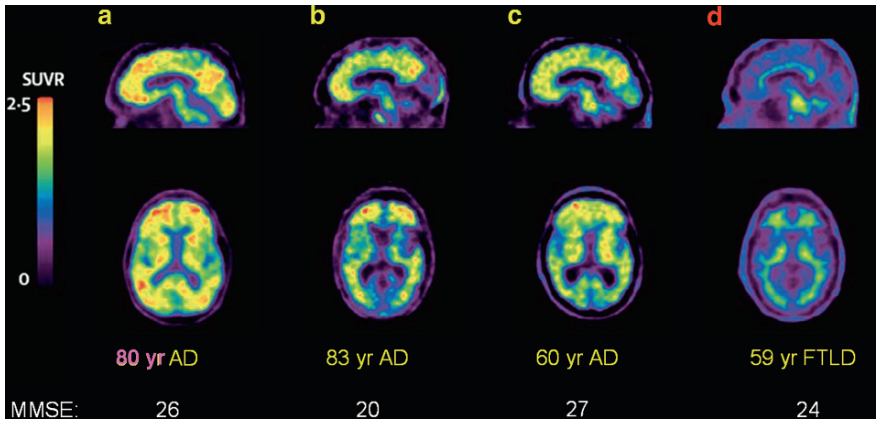

Fig. 16.27 ^{18}F-BAY94-9172 (Aβ ligand) PET images from three patients with AD and one patient with FTLD. There is cortical binding in the frontal, posterior cingulate/precuneus, and lateral temporal areas with relative sparing of the occipital and sensorimotor cortex in AD patients (**a**–**c**). By contrast, there is no cortical binding in the FTLD patient (**d**) (Rowe et al. 2008)

frontal and precuneus cortex. Another stilbene, [^{11}C]-SB13, has shown the same regional brain distribution pattern as PIB, when studied in the same population of AD patients and age-matched healthy controls (Verhoeff et al. 2004).

In summary, the potential applications of Aβ imaging agents include their use as diagnostic agents to detect cerebral β-amyloidosis, to help test the amyloid cascade hypothesis of AD, and to assist with the development of antiamyloid therapeutic drugs (Mathis et al. 2007 < Nordberg et al 2008). As diagnostic imaging markers in AD, PIB and other Aβ-PET molecular imaging probes depend on the ability to discriminate between AD and other forms of dementia. Some major issues and concerns need additional clinical studies to further validate the potential clinical utility of in vivo brain amyloid imaging.

16.3.1.3 Cholinergic System

The central role of the cholinergic system in the AD pathway is becoming increasingly significant. The cholinergic hypothesis implies that a degeneration of cholinergic neurons in the basal forebrain and the associated loss of cholinergic neurotransmission in the cerebral cortex and other brain areas contribute significantly to the deterioration in cognitive function seen in patients with AD (Bartus et al. 1982). These neurons express AChE, an enzyme responsible for the degradation of Ach. Also, in recent years, increasing evidence has emerged suggesting an interrelationship between the basal forebrain cholinergic neurotransmission and the metabolism of the amyloid precursor protein (APP). Significant improvement of cognitive function, relative to a placebo after therapy with acetylcholinesterase inhibitors (AChEIs) in AD provides support for the cholinergic hypothesis (Herholz et al. 2004). Abnormalities in the cholinergic system in AD include alterations in the Ach synthesis and receptor expression, and a decrease in nAChRs ($\alpha_4\beta_2$ subtype) are of particular interest.

With Ach analogs and substrates for AChE, [^{11}C] MP4A and [^{11}C]MP4P, reduced uptake has been observed in AD in all cortical areas, most severely in the occipital and temporal cortex, while uptake in basalis of Maynert is preserved, suggesting that cholinergic impairment begins in the cortical regions and affects the basal cell nuclei slowly, as a result of a "dying back" phenomenon (Fig. 16.28) (Kuhl et al. 1999; Heiss and Herholz 2006). The inhibition of acetylcholinesterase, which results from treatment with specific drugs, such as donepezil, can also be measured with these tracers (Kuhl et al. 2000). As discussed earlier, [^{11}C]epibatidine, is a highly specific ligand for AChE, but it is also very toxic and, therefore, not suitable for human studies.

Preliminary studies in humans with 6-[^{18}F]fluoro-A-85380 and 5-[^{123}I]iodo-A-85380 suggest that these tracers may have potential utility in assessing nAChRs (Fowler et al. 2003; Kulak et al. 2002). In a recent study (Sabri et al. 2008), 2-[^{18}F]fluoro-A-85380 was shown to be potentially useful in the diagnosis of patients at risk for AD (Fig. 16.29). Because of the extraordinary long acquisition time (>5 h) needed with this tracer, a new analog, (−)[^{18}F]norchloro-fluoro-homoepibatidine (NCFHEB) was investigated, which has shown twofold higher brain uptake and significantly shorter acquisition times. Therefore, NCFHEB should be a suitable radioligand for larger clinical investigations.

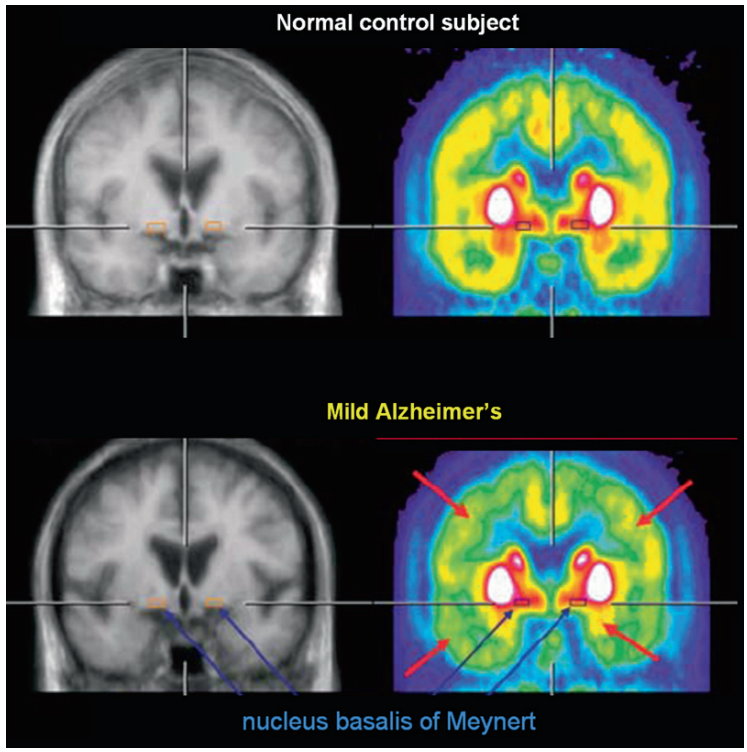

Fig. 16.28 Imaging acetylcholinesterase (AChE) activity in the brain using [^{11}C] MP4A-PET in mild-to-moderate AD. Reduction in cortex and amygdala with preserved activity in basal forebrain suggests a dying back of cholinergic neurons rather than initial loss of cell bodies (Heiss and Herholz 2006)

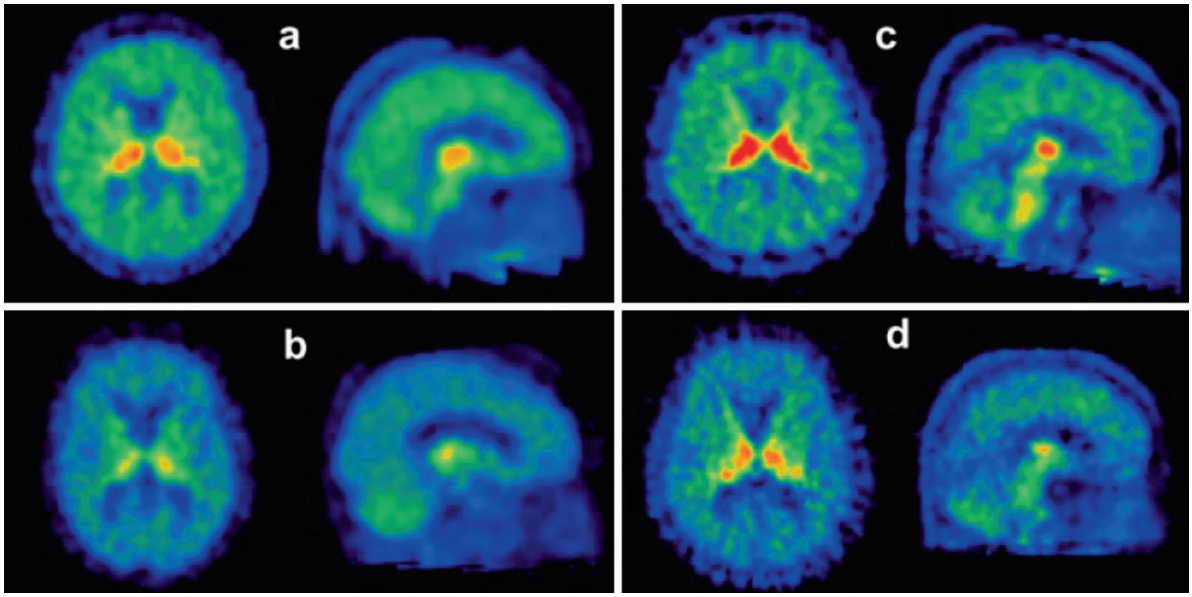

Fig. 16.29 Imaging nicotinic acetylcholine receptors (nAChR) using [^{18}F]fluoro-A-85380-PET in a normal aged healthy control (**a**), an AD patient (**b**), and two MCI patients (**c** and **d**). Patients **b** and **d** show significant reductions in binding potential compared to normal control (**a**), while MCI patient (**c**) is comparable to normal control (**a**) in all brain areas (Sabri et al. 2008)

A wide variety of other receptor binding radiotracers have also been used to study AD. An analog, [^{11}C] *R*-PK11195 binds to the peripheral benzodiazepine receptors within the outer mitochondrial membrane of the activated microglia, which are mediators of CNS inflammation (90). One hypothesis for the pathophysiology of AD is that the activated microglia may produce cytokines that in turn produce neuronal damage, or, perhaps, mediates the neuronal damage caused by the β-amyloid protein. Consistent with this hypothesis are the salutary effects noted with anti-inflammatory drugs in patients with AD and the fact that [^{11}C]*R*-PK11195 binding is significantly increased in the temporal cortex of patients with AD compared to that of age matched control subjects (Gilman et al. 1995).

16.3.2 Parkinson's Disease

PD is the prototypic movement disorder described almost 200 years ago by James Parkinson and is characterized by a constellation of motor (slowness of movement, muscular rigidity, tremor, and postural instability) and nonmotor symptoms (cognitive dysfunction and psychiatric features) that inexorably progress over time (Seibyl 2008). Idiopathic PD is the most common movement disorder among a spectrum of diseases with common features, but different causes, prognosis, and clinical course. Under normal circumstances, nerve cells in the substantia nigra communicate with other cells in the nearby striatum (the caudate nucleus and putamen) by releasing dopamine at nerve terminals in that region. Many neurons in the substantia nigra are destroyed in individuals with PD causing slowed movements, rigidity, and tremors. The discovery in the late 1950s that the level of dopamine was decreased in the brains of Parkinson's patients was followed in the 1960s by the successful treatment of this disorder by administration of the drug L-DOPA (levodopa), which is converted to dopamine in the brain. Levodopa is now combined with another drug, carbidopa that reduces the peripheral breakdown of levodopa, thus allowing greater levels to reach the brain and reducing side effects.

The discovery in the late 1970s that the neurotoxin, 1-methyl-4-phenyl-1,2,3,6-tetrahydropyridine (MPTP), can cause parkinsonism in drug addicts has stimulated intensive research on the causes of the disorder (Herholz et al. 2004). MPTP was found to be converted in the brain to a substance that destroys dopamine neurons, thus, the disturbance of dopamine synthesis is the hallmark of PD.

The diagnosis of PD is primarily made on the basis of clinical assessment and becomes difficult by the variability of the disease presentation, rate of progression, and response to medications. Morphological imaging techniques, such as CT and MRI, may help to exclude other diseases that may lead to Parkinsonism. The other important neurodegenerative diseases that present, clinically, as Parkinsonian syndromes, often in combination with dementia, include progressive supranuclear palsy (PSP), corticobasal degeneration (CBD), dementia with Lewy bodies (DLB), Alzheimer's and Huntington's dementia, and other hereditary neurodegenerative disorders. In most of the patients with PD, FDG-PET is generally normal and is, therefore, not necessarily useful clinically. However, in the last two decades, a number of PET and SPECT molecular imaging techniques to assess presynaptic dopaminergic function have demonstrated significant potential for providing a confirmative diagnosis of PD. These neuroimaging biomarkers in movement disorders may also serve as tools for the evaluation of novel therapeutics and as a powerful means for describing pathophysiology by revealing in vivo changes at different stages of disease and within the course of an individual patient's illness. A number of radiolabeled molecular imaging probes (Fig. 16.30) based on the dopaminergic system are available for imaging studies in PD and other movement disorders. The specific PET or SPECT radiotracer for use in movement disorders depends on the clinical or research question to be addressed by imaging. All presynaptic markers may have utility for the qualitative clinical evaluation of regional striatal signal loss to describe the presence or absence of a dopaminergic deficit in the context of making a diagnosis of PD or related disorder. If the goal is measurement of the progression of disease with serial imaging in a large clinical trial, then a tracer with a highly reproducible, semiquantitative, or quantitative imaging outcome is necessary (Seibyl 2008).

16.3.2.1 Dopamine Synthesis

In 1983, [^{18}F]FDOPA-PET was introduced to image dopamine synthesis in vivo. In normal subjects, the images show higher tracer uptake in the striatum (caudate and putamen) and the midbrain, while uptake in the cerebral cortex and cerebellum is much lower

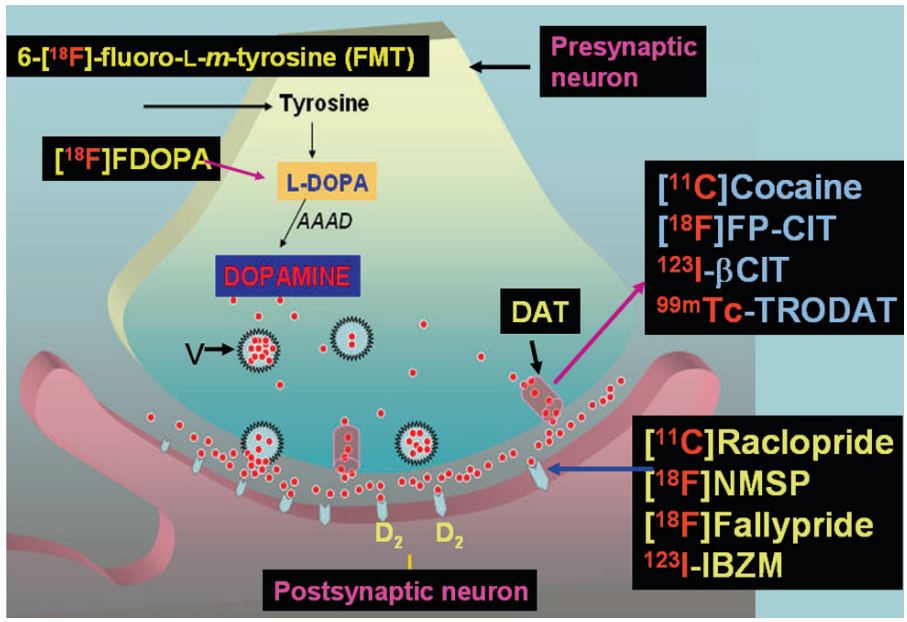

Fig. 16.30 PET and SPECT radiotracers for imaging dopaminergic system

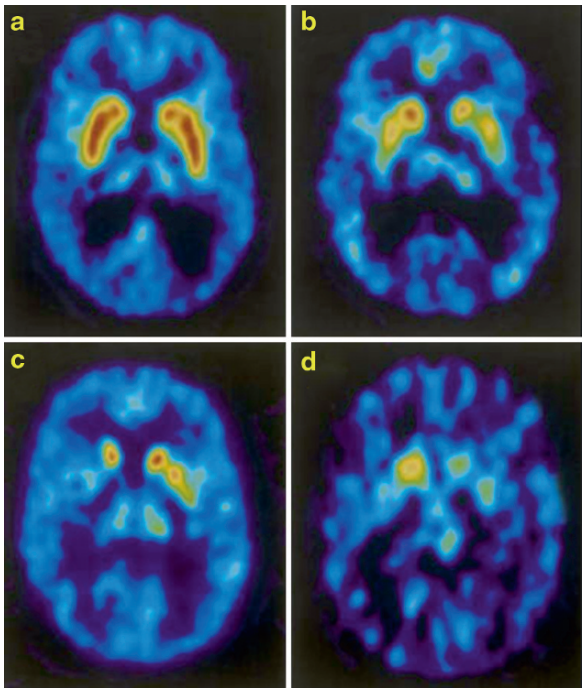

Fig. 16.31 [18F]FDOPA-PET to image presynaptic dopaminergic neurons in basal ganglia. Representative midstriatal transaxial images through the caudate and putamen of a healthy volunteer (**a**) and patients with unilateral PD (**b**), moderate severity PD (**c**), and severe PD (**d**) (Fischman 2005)

(Fig. 16.31). In patients with PD, the tracer uptake and retention in the striatum are reduced, most markedly on the opposite side of the major motor signs (Garnett et al. 1984). The posterior parts of the putamen are most affected and the heads of caudate nuclei are the least affected, which is consistent with preferential degeneration of dopaminergic neurons in the caudal and mediolateral part of the substantia nigra pars compacta (Fischman 2005). This typical, differential intrastriatal distribution of reduced uptake is often referred to as the *rostrocaudal gradient*. While FDOPA images are useful to assess dopamine synthesis in presynaptic neurons of patients with PD, it is not possible to distinguish between PD and other disorders with Parkinsonian symptoms on the basis of FDOPA studies alone, because many of these disorders are associated with some degree of decreased striatal FDOPA uptake (Herholz et al. 2004). FDOPA is also not an ideal radiotracer to study dopamine synthesis, since the quantitative analysis with FDOPA-PET in humans is flawed by the presence of radioactive metabolites, which cross the BBB and contribute significantly to the radioactivity uptake in the brain (Firnau et al. 1988). 6-[18F]-fluoro-L-*m*-tyrosine (FMT) is regarded as an alternative tracer to FDOPA for the visualization of dopaminergic presynaptic integrity because of its lower in vivo metabolism. Following the synthesis of dopamine from L-DOPA, dopamine is transported and stored in the vesicles in the presynaptic neurons via specific $VMAT_2$ receptors. Because of degeneration of presynaptic neurons in PD, there is a significant reduction in these receptors. [11C]DTBZ has been shown to be useful to image the reduction of

$VMAT_2$ transporters in patients with PD and the reduction of these transporters is more severe than FDOPA striatal uptake (Frey et al. 2001; Kumar et al. 2003).

16.3.2.2 Dopamine Transporters

As discussed earlier, following release of dopamine into a synapse, dopamine is transported back into the presynaptic neuron via DATs. Therefore, DATs are important in the regulation of synaptic concentrations of dopamine. Several PET and SPECT radiopharmaceuticals based on tropane (cocaine) derivatives have been used to study and quantify brain DATs in patients with PD (Marshall and Grosse 2003; Ravina et al. 2005; Seibyl 2008). Among the ^{18}F labeled analogs, FP-CIT and FE-CNT have been evaluated in patients with PD (Ma et al. 2002). For example, FE-CNT-PET has shown to provide high striatum/cerebellum ratios and had the most favorable kinetics for quantitation of DATs (Davis et al. 2003). However, a recent preclinical investigation in a rat model suggests that a polar metabolite of FE-CNT may complicate quantitative assessment of DATs in human studies (Zoghbi et al. 2006). [^{18}F] FP-CIT is a high affinity cocaine analog with fast kinetics and high signal-to-noise ratios and is suitable for PET neuroimaging (Ma et al. 2002; Robeson et al. 2003). The initial studies have indicated that DAT imaging might be more sensitive in detecting early stage of PD than FDOPA imaging (Eshuis et al. 2006). A recent study in patients with PD at various clinical stages has indicated that FP-CIT-PET can serve as a suitable biomarker to represent the severity of PD in early and advanced stages (Fig. 16.32) (Wang et al. 2006).

A number of tropane analogs as radiotracers for SPECT, such as ^{123}I-βCIT, ^{123}I-FP-CIT, ^{123}I-Altropane, and ^{99m}Tc-TRODAT, have been investigated to assess the diagnostic potential for imaging the dopaminergic degeneration in patients with PD. ^{123}I-βCIT-SPECT images (Fig. 16.33) have been useful for the visual evaluation of the integrity of the dopaminergic projections to striatum in patient with PD (Jennigs et al. 2004). Similarly, ^{99m}Tc-TRODAT-1 also binds with high affinity to the DAT, allowing for SPECT imaging of the striatum in patients with PD (Kung et al. 2003a; Mozley et al. 2000; Chou et al. 2004).

In general the DAT ligands appear to provide a more sensitive indicator of dopaminergic degeneration than FDOPA. During the past decade, neuroimaging biomarkers have served in movement disorders as clinically available diagnostic agents (Europe), tools for evaluation of novel therapeutics, and powerful means for describing pathophysiology by revealing in vivo changes at different stages of disease and within the course of an individual patient's illness. However, challenges remain in the ideal application of neuroimaging in the clinical algorithms for patient assessment and management (Seibyl 2008).

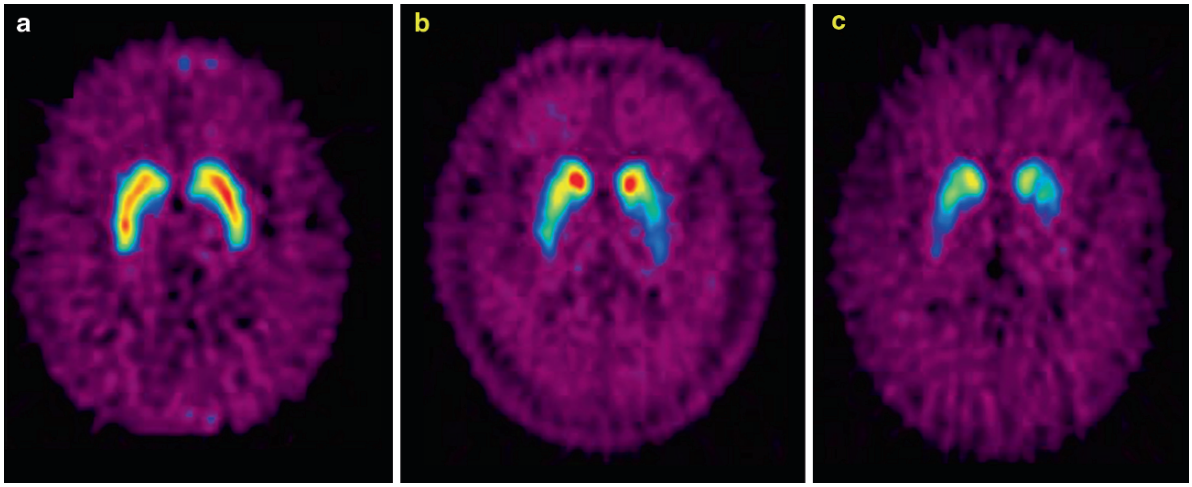

Fig. 16.32 [^{18}F]FP-CIT-PET to image dopamine transporter (DAT) density in patients with PD. Compared to the healthy control (**a**), the two PD patients (patient (**b**) with early PD with HY stage I and patient (**c**) with advanced PD with HY stage IV) display progressive reduction in striatal DAT binding (Wang et al. 2006)

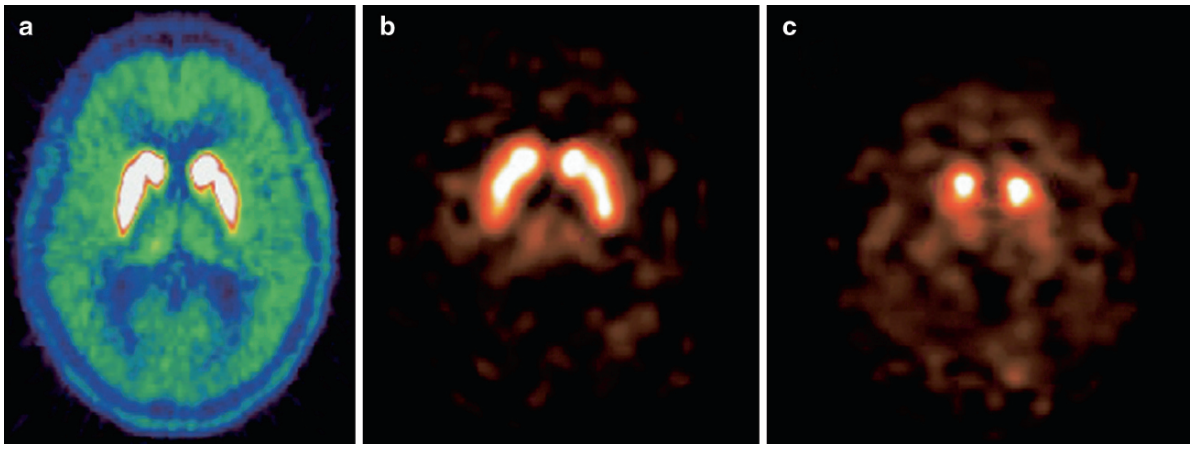

Fig. 16.33 ^{123}I-βCIT-SPECT for imaging dopamine transporters in patients with PD. ^{123}I-βCIT uptake in a patient with PD (**c**) shows significant reduction in striatal uptake compared to a healthy control (**b**). FDOPA-PET image of basal ganglia in a healthy control (**a**) is shown for comparison of SPECT image quality. (Seibyl 2008)

16.3.3 Epilepsy

Epilepsy is a common neurological disorder that is characterized by recurrent, unprovoked seizures. About 60–70% of patients experience focal or partial seizures and 30–40% generalized seizures (Newberg and Alavi 2005). Epilepsy is controlled with medication in approximately 70% of the cases. When seizures are medically intractable, resection of the epileptogenic cortex may be considered (Goffin et al. 2008). The seizure-onset zone is the region in which the seizures actually originate, while the epileptogenic zone is a theoretical construct, which is defined in terms of different cortical zones (Goffin et al. 2008).

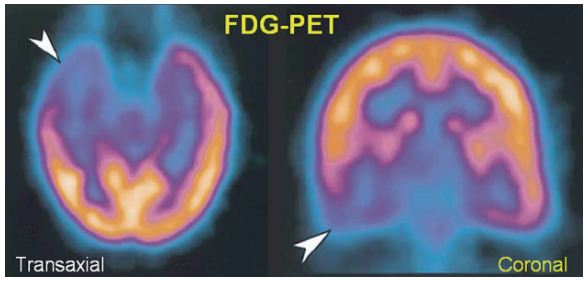

Fig. 16.34 FDG-PET in a patient with temporal lobe epilepsy. The images show markedly reduced glucose metabolism in the right temporal lobe (arrow) in transaxial and coronal views (Casse et al. 2002)

16.3.3.1 Blood Flow and Metabolism

Patients with complex partial seizures (epilepsy that leads to temporary impairment, but not loss of consciousness) may be referred for functional brain imaging studies to assess the ictal perfusion or interictal glucose metabolism. During the epileptic activity, a hyperperfusion of the seizure onset zone occurs because of an autoregulatory response to the local neuronal hyperactivity. When a SPECT blood flow tracer (^{99m}Tc-HMPAO or ^{99m}Tc-ECD) is injected intravenously immediately after the start of a seizure, the ictal SPECT images reflect the hyperperfusion changes in the early phase of the seizure. However, if the tracer is injected after the seizure is terminated, hypoperfusion in the seizure onset zone can be observed. Ictal-SPECT is the only imaging modality that can define the ictal onset zone in a reliable and consistent manner. Brain glucose metabolism, as a measure of neural activity, can be studied with FDG-PET, which identifies cerebral hypometabolism characterizing epileptogenic sites (Fig. 16.34). FDG-PET is useful for presurgical planning in most temporal lobe epilepsy (TLE) patients. However, different antiepileptic drugs have shown to affect the cerebral glucose metabolism to varying degrees, with phenobarbital being a greater depressant (up to 37%) than valproate, carbamazepine, or phenytoin (Casse et al. 2002).

16.3.3.2 Neuroreceptors

Hyperexcitability, synapse reorganization, and imbalance between inhibitory and excitatory synapses are three dysfunctions characterizing the epileptogenic zone. GABA is the main inhibitory neurotransmitter in the brain and maintains the inhibitory tone that counterbalances neuronal excitation. Evidence from experimental and clinical studies indicates that GABA plays an important role in the mechanism and treatment of epilepsy (Treiman 2001). Several lines of evidence suggest that serotonin (5-HT) may also have an anticonvulsant effect through activation of the 5-HT_{1A} receptor, because activation of this receptor affects the release and activity of other neurotransmitters such as glutamate, dopamine, and GABA (Theodore 2004; Goffin et al. 2008).

In the pathogenesis of epilepsy, the $GABA_A$ receptor, also known as the central benzodiazepine-receptor (BZR), is the most studied neuroreceptor with [^{11}C]flumazenil (FMZ). In patients with TLE, arising from amygdala/hippocampal regions, a localized reduction of FMZ binding in the mesial temporal lobe is seen, in contrast to the more extensive hypometabolic changes seen with FDG-PET. The reduction in FMZ binding is proportional to the neuronal loss on histopathology and may be more sensitive than MRI in the detection of hippocampal sclerosis (Szelies et al. 2002). Also, in extratemporal epilepsies FMZ-PET shows a more localized reduction in receptor binding in the region of the cortical focus compared to the more extensive defects seen with FDG (Casse et al. 2002). Flumazenil is a biochemical marker of epileptogenicity and neuronal loss; BZR-density changes are more sensitive than FDG-PET in detecting hippocampal sclerosis or microdysgenesis. BZR studies have also been useful in the selection of patients for targeted surgery and for predicting outcome of these procedures (Heiss and Herholz 2006). The availability of [^{18}F]flumagenil may provide greater opportunity to investigate the role of BZRs in epilepsy. [^{123}I]iomazenil (IMZ) brain SPECT has also been used to detect epileptic foci, especially when surgical intervention is considered. In a recent study of patients with intractable epilepsy, IMZ-SPECT brain images, following MRI-based corrections for the partial volume effect (PVE), has shown improved sensitivity and specificity for the detection of cortical epileptogenic foci (Kato et al. 2008) (Fig. 16.35).

On the basis of 5-HT_{1A} receptor antagonists, [^{18}F]FCWAY and [^{11}C]WAY-100635, several studies of patients with TLE have demonstrated a reduced serotonin receptor binding in the TLE foci (Toczec et al. 2003; Goffin et al. 2008). Compared to normal subjects, the epileptic patients have shown a decreased binding of another $5HT_{1A}$ receptor antagonist, [^{18}F]MPPF (Fig. 16.36), suggesting a decrease in the availability of 5-HT_{1A} receptors (Merlet et al. 2004). This decrease is highly correlated to the degree of epileptogenicity of cortical areas explored by intracerebral recordings, and does not reflect only pathological changes or neuronal loss in the epileptic focus.

16.3.4 Cerebrovascular Disease

Acute cerebrovascular disease (CVD), the cause of clinical syndromes of stroke is the most common neurological

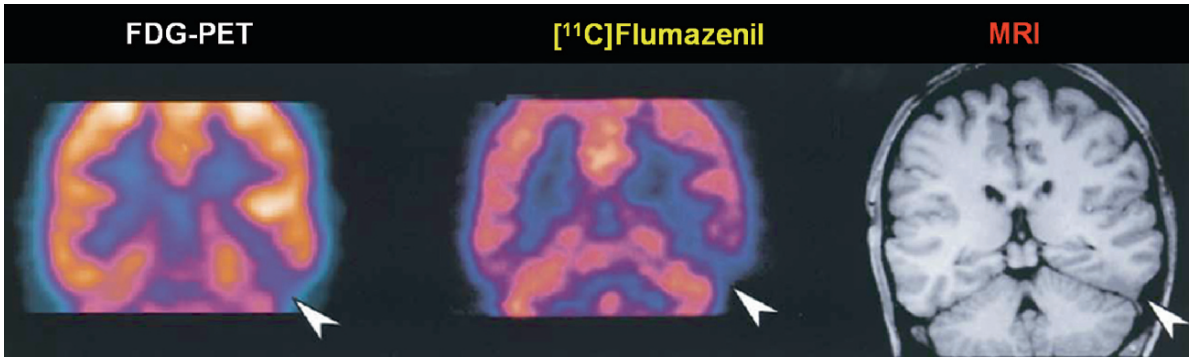

Fig. 16.35 [^{11}C]Flumazenil-PET to image benzodiazepine-receptor (BZR) density in extratemporal epilepsy. Interictal FDG-PET shows reduced glucose metabolism in the left occipital lobe (*arrow*) and [^{11}C]flumazenil PET also shows reduced BZD density in the same region, while MRI shows a poorly defined cortical margin consistent with dysplasia in this region (Casse et al. 2002)

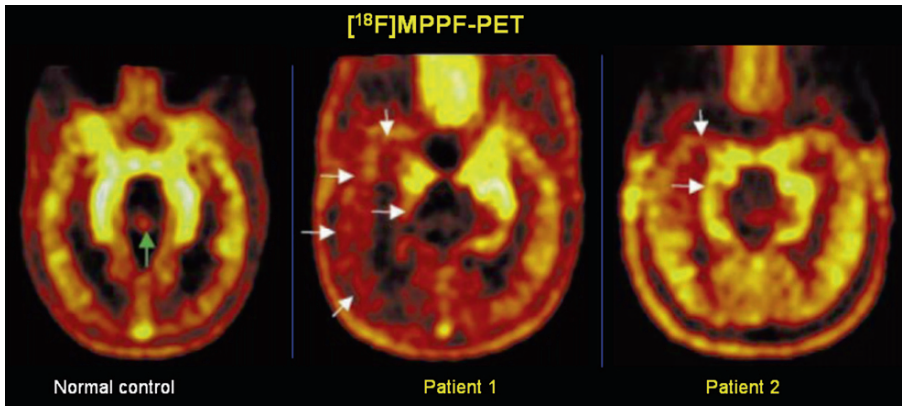

Fig. 16.36 [^{18}F]MPPF-PET to image 5-HT$_{1A}$ receptor binding and intracerebral activity in temporal lobe epilepsy. *White arrows* indicate asymmetries in FMPPF binding in patients 1 and 2. Patient 1 shows decreased binding in left mesiotemporal and lateral temporal structures, as well as in extratemporal regions (insula, operculum and frontal regions), while patient 2 shows a more focal asymmetry, with a binding decrease in the right hippocampus, part of the right inferior temporal gyrus, and in the right temporal pole (Merlet et al. 2004)

disorder. There are three main etiological categories: the ischemic stroke (70–80%), spontaneous intracerebral hematoma (10–20%), and subarachnoid hemorrhage (5–10%) (Herholz and Heiss 2004). The cause of ischemic stroke is a severe and usually sudden decrease of CBF (<15 mL 100 g^{-1} min^{-1}), mostly because of the atherothrombotic or embolic occlusion of a supplying artery. A central core of dense ischemia or necrosis (<12 mL 100 g^{-1} min^{-1}) surrounded by an area of reduced blood flow (12–22 mL 100 g^{-1} min^{-1}), where function is impaired but morphology is preserved, is known as *penumbra*. Metabolically an ischemic stroke is characterized by a condition known as *misery perfusion*, which is a mismatch of relatively well preserved oxygen metabolism due to increased oxygen extraction and severely reduced CBF. However, continued decline in CBF leads to a decline in oxygen delivery and metabolism (the onset of ischemia). Severe and prolonged compromise in blood flow results in infarction of brain tissue leading to a decline in oxygen extraction (onset of luxury perfusion). The role of imaging techniques is (a) to determine the regional CBF quantitatively and (b) to identify precisely the status and extent of penumbra.

16.3.4.1 Assessment of CBF

In 2007, the National Institute of Health, in conjunction with the American Society of Neuroradiology and the Neuroradiology Education and Research Foundation, sponsored a research symposium entitled *Advanced NeuroImaging for Acute Stroke Treatment* (Wintermark et al. 2008). The main goals of the meeting were to assess state-of-the-art practice in terms of acute stroke imaging research and to propose specific recommendations regarding (1) the standardization of perfusion and penumbral imaging techniques, (2) the validation of the accuracy and clinical utility of imaging markers of the ischemic penumbra, and (3) the validation of imaging biomarkers relevant to clinical outcomes.

A number of SPECT radiopharmaceuticals, such as ^{123}I-IMP, ^{99m}Tc-HMPAO, and ^{99m}Tc-ECD, have shown clinical utility for the qualitative assessment of rCBF. However, only PET based methods, using intravenous administration of [^{15}O]H_2O and inhalation of gases, such as [^{15}O]O_2 or [^{15}O]CO_2, can provide quantitative assessment of both rCBF and the extent of penumbra. Because of the potential for postischemic hyperperfusion (luxury perfusion), determination of the rCBF alone may not be sufficient to assess the area of penumbra, which is essential for optimal therapeutic management. However, PET images obtained with multiple radiotracers can demonstrate the value of PET in the assessment of rCBF, $CMRO_2$, and OEF in a patient with acute cerebral ischemia (Jacobs et al. 2005). The area with decreased rCBF, but increased OEF, represents the functionally viable tissue, the penumbra (Fig. 16.37).

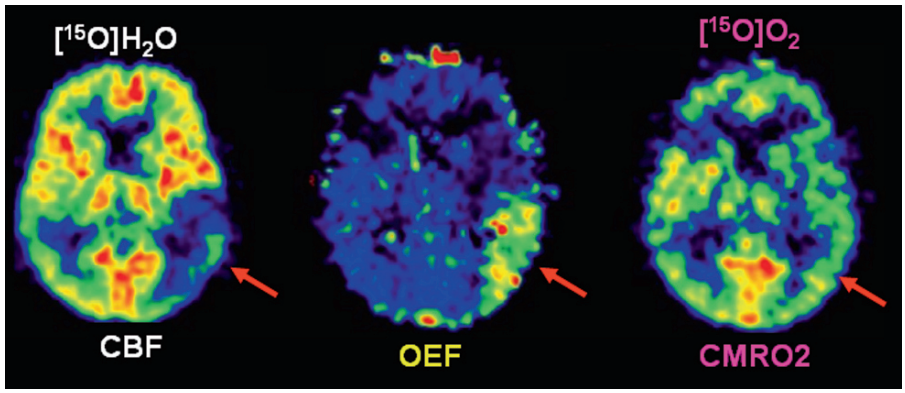

Fig. 16.37 Assessment of acute cerebral ischaemia. Cerebral blood flow (CBF) measured by [^{15}O]H_2O-PET demonstrates hypoperfusion in the posterior portion of the middle cerebral artery (MCA) territory. The cerebral metabolic rate of oxygen (CMRO2) as measured by [^{15}O]O_2-PET is still intact. On the basis of these two studies, the oxygen extraction fraction (OEF) shows relative increase indicating that the hypoperfused tissue is functionally disturbed but still viable, which is the classic definition of penumbra (Jacobs et al. 2005)

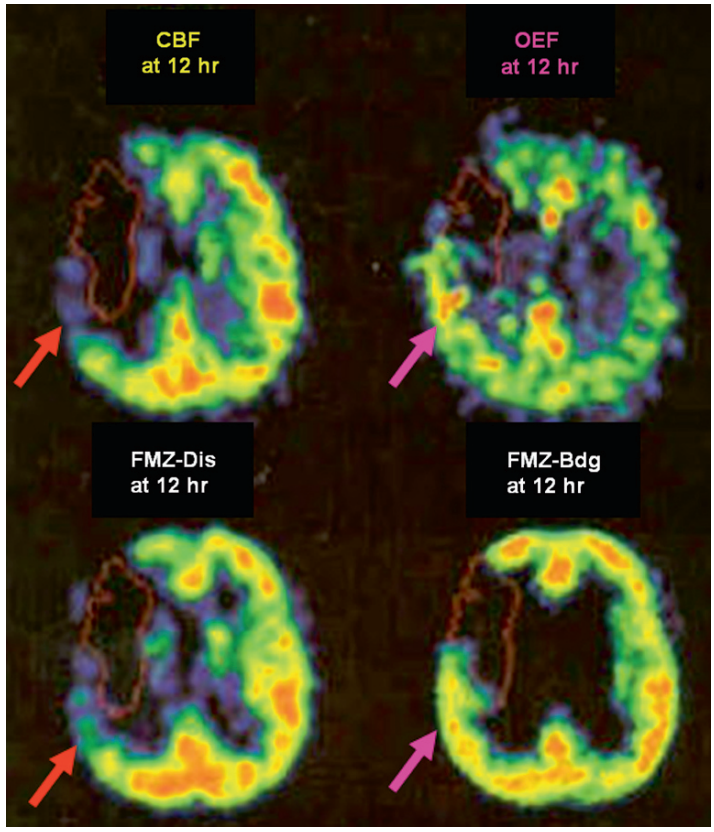

Fig. 16.38 [^{11}C]Flumazanil-PET for the precise identification of the status and extent of penumbra in patients with acute cerebral ischemia. FMZ-PET images showing early distribution (FMZ dis at 12 h) clearly identify the area of decreased cerebral perfusion. The delayed images (FMZ bdg at 13 h) reflect FMZ binding to the central benzodiazepine receptors and identify the area of penumbra as shown by OEF (Herholz et al 2004)

16.3.4.2 GABA Receptor Imaging

GABA receptors are very sensitive to ischemic damage because these receptors are expressed in high levels throughout the intact viable cortical neurons. Radiotracers, such as [^{11}C]Flumazenil, [^{18}F]Flumazenil, and [^{123}I]iomazenil, which bind to GABA receptors can be used as markers of neuronal integrity. The validity of this approach has been documented in patients with acute ischemic stroke (Herholz and Heiss 2004; Saur et al. 2006) by direct comparison with MRI or PET imaging studies of rCBF and OEF. The early images (10–20 min) reflect the distribution volume and provide a measure of rCBF, while the delayed images (at 1 h) represent the GABA receptor bound activity and provide a measure of the extent of the penumbra (Fig. 16.38).

16.3.4.3 Hypoxia Imaging

In ischemic stroke, the ischemic penumbra is likely to be hypoxic in nature. As a result, the hypoxic tissue can be identified using a nitroimidazole compound, such as [^{18}F]fluoromisonidazole (FMISO), which is trapped within the hypoxic cells after entering the cells by passive diffusion. Subsequently, FMISO is reduced by nitroreductase enzymes. Under normoxic conditions, the parent compound is regenerated by reoxidation. However, under hypoxic conditions reoxidation is prevented, additional reduction occurs, and the resulting metabolites are trapped by binding to intracellular molecules. Because trapping of the compound depends on active metabolism, no trapping occurs in the necrotic tissues (Read et al. 1998). FMISO-PET images performed within 4 h following acute ischemia clearly identify the hypoxic tissue as shown in Fig. 16.39 (Markus et al. 2002).

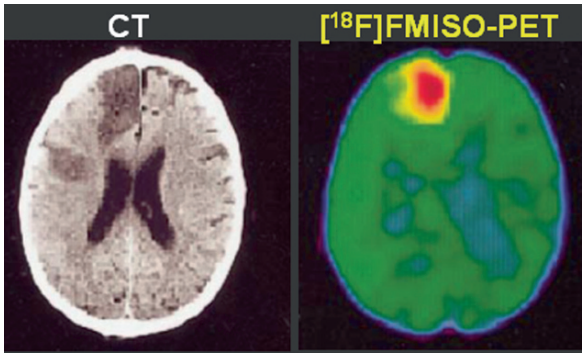

Fig. 16.39 [^{18}F]FMISO-PET to identify hypoxic tissue following acute cerebral ischemia. FMISO-PET performed 3.5 h after stroke onset, while the corresponding CT image performed on day 7 delineates the final infarct (Markus et al. 2002)

16.4 Psychiatric Disorders

The pathophysiological alterations in most of the neurological disorders have been well documented by morphological imaging studies (CT and MRI) and postmortem histopathological examination. In contrast, psychiatric diseases, such as depression, schizophrenia, anxiety, and addiction, can be due to functional abnormalities in the brain rather than significant structural abnormalities. In the last three decades, brain functional imaging studies of rCBF and $rCMR_{glu}$ based on PET have provided considerable insights into the understanding of psychiatric diseases. However, these functional imaging studies of blood flow and energy metabolism have not been useful for developing either well defined image based diagnostic criteria, or to assess therapeutic response of various psychopharmacological agents. Since neuronal firing and signal transmission are the basis for brain function, molecular imaging of neurotransmitter–neuroreceptor interaction based on PET and SPECT radiotracers may be the most appropriate noninvasive imaging modality to study psychiatric disorders. Neuroreceptor imaging can play an important role in quantifying the relationship between receptor occupancy, drug blood levels, and oral dose and may contribute to both therapeutics and drug development by rapid identification of the likely therapeutic dose range (compared with conventional parallel group dose comparisons or dose ranging studies) (Parsey and Mann 2003).

16.4.1 Schizophrenia

Schizophrenia is considered to reflect changes in the brain, possibly caused by disease or injury at the time of birth, and a genetic disposition that may be exacerbated by environmental stress. Marked by disturbances in thinking, emotional reactions, and social behavior, schizophrenia usually results in chronic illness and

personality change. The positive symptoms include delusions and hallucinations, while the negative and cognitive deficits may involve attention and memory, and are associated with thought disorder.

16.4.1.1 Biology of Schizophrenia

The classical dopamine hypothesis formulated more than 35 years ago proposes that schizophrenia is associated with hyperactivity of dopaminergic neurotransmission. Until recently, the evidence supporting the dopamine hypothesis has been indirect: medications that share the ability to improve the psychotic symptoms of schizophrenia share the property of blocking dopamine D_2 receptors, and drugs that increase dopamine levels (such as amphetamine and cocaine) can both provoke psychotic symptoms in otherwise healthy individuals and worsen psychotic symptoms in patients with schizophrenia (Zipursky et al. 2007). The advent of neuroreceptor imaging with PET and SPECT has provided a new opportunity to systematically investigate the biology of schizophrenia.

Initial PET and SPECT ligand studies have focused on determining whether patients with schizophrenia have increased numbers of striatal dopamine (specifically D_2) receptors. Studies of never-medicated schizophrenia patients, using the PET D_2 ligands, [^{11}C] raclopride and *N*-[^{11}C]methylspiperone, and the SPECT ligand [^{123}I]IBZM, have not yielded consistent results (Frankle and Laruelle 2002). The discrepant results have been attributed to differences in the radiotracer binding to D_2 receptors (reversible vs irreversible or high vs. moderate affinity) or to the competition by the synaptic levels of endogenous dopamine.

Several drugs are known to alter the brain dopamine levels. For example, cocaine, cannabis, and stress can increase dopamine levels. Amphetamine causes the release of dopamine from the presynaptic terminals into the synapse. The tyrosine hydroxylase inhibitor AMPT depletes the dopamine levels in the synapse. Studies with ^{123}I-IBZM and [^{11}C]raclopride have made two important observations:

(a) Prior administration of amphetamine to unmedicated schizophrenic patients has shown a greater average decreases in D_2 receptor binding, compared control subjects (Laruelle et al. 1996; Breier et al. 1997).
(b) D_2 receptor availability increases after AMPT administration and is greater in patients, than in control subjects, after dopamine is depleted, but not before (Abi-Dargham et al. 2000b). These findings suggest that the increased sensitivity of the dopamine system in schizophrenia patients is malleable and may reflect either the relapsed state or, perhaps, risk for relapse. The contemporary view of the role of dopamine is that subcortical mesolimbic DA projections may be hyperactive (resulting in positive symptoms) and the mesocortical DA projections to the PFC may be hypoactive (resulting in negative symptoms and cognitive impairement) (Laurelle et al. 2002)

16.4.1.2 Dopamine Receptor Occupancy and Antipsychotic drugs

PET and SPECT dopamine D_2 receptor imaging studies clearly demonstrated that clinical dosages of antipsychotic medications block striatal D_2 receptors (Fig. 16.40) (Farde et al. 1992; Kapur and Remington 2001). Treatment of schizophrenia patients with a range of antipsychotic medications resulted in the blockage of 65–90% of striatal D_2 receptors. Further, patients with acute extrapyramidal symptoms were shown to have higher levels of D_2 receptor occupancy. Although it is clear that clinical dosages of all first generation antipsychotics (FGAs), such as haloperidol, result in the blockage of a substantial percentage of D_2 receptors, it is not known whether a threshold level of blockage would be sufficient for antipsychotic action (Zipursky et al. 2007). These studies also clearly demonstrate that levels of D_2 receptor occupancy, associated with clinical response, can be achieved with dosages of FGAs that are, in some cases, only 5–10% of those used in common clinical practice. PET studies with the second generation of antipsychotics (SGAs), such as clozapine and risperidone have demonstrated that therapeutic dosages result in lower levels of D_2 occupancy, in the range of 38–63% (Farde et al. 1992), suggesting that continuous high levels of binding of the antipsychotic drug at the D_2 receptor are not required for ongoing antipsychotic efficacy.

Further, PET and SPECT radioligand research has provided evidence that patients with schizophrenia have a modest increase in D_2 receptor numbers, a substantial increase in endogenous dopamine, and that intermittent blockade of D_2 receptors is necessary to facilitate an antipsychotic response. Additional work is

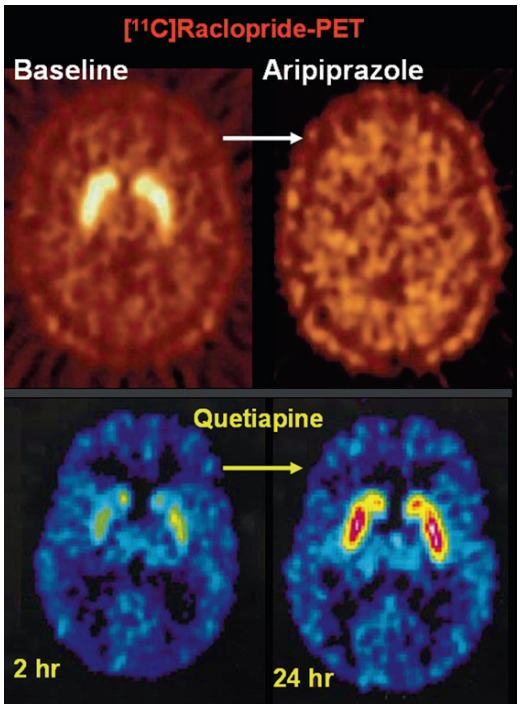

Fig. 16.40 Dopamine D_2 receptor imaging with [^{11}C] Raclopride-PET in patients with schizophrenia and the effect of antipsychotic drug treatment. The images (*top*) show 95% receptor occupancy (*compared to baseline*) after the administration of aripiprazole at a dose of 30 mg per day for 14 days (Hammoud et al. 2007). The images (*bottom*) show transient decrease in receptor occupancy (64%), only 2 h after a single dose of quetiapine (400 mg), but 24 h later, a repeat PET study shows 0% occupancy of dopamine D2 a receptors (Kapur et al. 2000)

required to determine what levels of occupancy are required and for what amount of time, why a minority of patients fail to respond well despite substantial D_2 occupancy, and how other domains of symptomatology may relate to medication binding at dopamine and nondopamine neuroreceptors (Zipursky et al. 2007).

16.4.2 Depression

The diagnosis of major depressive disorder (MDD) requires a distinct change of mood, characterized by sadness or irritability, accompanied by at least several psychophysiological changes, such as disturbances in sleep, appetite, or sexual desire, constipation, loss of the ability to experience pleasure in work or with friends, crying, suicidal thoughts, and slowing of speech and action. These changes must last a minimum of two weeks and interfere considerably with work and family relations (Belmaker and Agam 2008; Meyer 2008).

Several SPECT and PET studies have documented significant regional differences in the CBF and glucose metabolism of patients with MDD. In acute major depression, imaging studies have primarily identified the prefrontal cortex, the temporal lobes, the cingulated cortex, and the related parts of the basal ganglia and thalamus, as an important neural correlate (Herholz et al. 2004). Also, both blood flow and glucose metabolic rate in the frontal cortex have been found to inversely correlate with disease severity. Patterns of [^{18}F]FDG and [^{15}O]H_2O uptake in MDD tend to demonstrate overactivity of regions that generate mood and underactivity of regions related to cognition (Meyer 2008).

The monoamine hypothesis of depression postulates a deficiency in serotonin or norepinephrine neurotransmission in both serotonergic and noradrenergic neurons in the brain. Cessation of the synaptic action of these neurotransmitters occurs by means of both reuptake through the specific serotonin and norepinephrine transporters and feedback control of release through the presynaptic regulatory autoreceptors for serotonin and norepinephrine. The hypothalamic–pituitary–cortisol hypothesis postulates that abnormalities in the cortisol response to stress may underlie depression. However, the clinical data do not support these hypotheses since monoamine-based antidepressants are most effective in patients with severe depression, when cortisol levels remain high after the administration of dexamethasone (Belmaker and Agam 2008).

16.4.2.1 Role of Serotonin Receptors and Transporters

If the original monoamine theory is true, one would expect increased 5-HT_2 receptor density in untreated subjects with depression, because extracellular-serotonin (5-HT) levels are low. PET studies of 5-HT_{2A} receptors, using [^{18}F]setoperone in untreated subjects suffering from depression, have documented no difference in receptor status during the depressive episodes. However, higher 5-HT_{2A} binding potential has been found in depressed patients with severe pessimism (Meyer et al. 2003). The regional 5-HT transporter binding potentials, based on [^{11}C]DASB-PET studies, are also higher during depressive episodes with more severe pessimism. These results may be interpreted to

mean that greater monoamine transporter density facilitates monoamine loss, which in turn contributes to greater severity of the depressive symptoms (Meyer et al. 2001a). Radioligand neuroimaging studies have also advanced the monoamine theory of MDD to explain the chronic loss of particular monoamines, such as serotonin, norepinephrine, and dopamine, which occurs to a greater extent when particular symptoms are more severe. In addition, neuroimaging has also identified mechanisms of monoamine loss, including greater monoamine metabolism, and excessive monoamine transporter density in the presence of monoamine depleting processes (Meyer 2008).

Antidepressants bind to the 5-HT transporter and raise extracellular serotonin levels of 5-HT.Serotonin transporter imaging with, [^{11}C](+)McN5652, [^{11}C] DASB, ^{123}I-β-CIT, and 123I-ADAM has made it possible to quantify more precisely the degree to which commonly prescribed antidepressant medications bind to the transporter at different dosages (Meyer et al. 2004). The first SSRI occupancy study with [^{11}C] DASB-PET reported an 80% occupancy in multiple regions after 4 weeks of paroxetine at 20 mg/day and citalopram at 20 mg/day (Meyer et al. 2001b). Similar occupancy levels have been reported with other antidepressants such as fluvoxamine, fluoxetine, sertraline, and venlafaxine (Suhara et al. 2003b; Meyer et al. 2004). These studies demonstrate that receptor ligand imaging can not only inform us about that mechanisms that may underlie major depression and its symptoms, but has also provides clinically relevant information about how antidepressants should be prescribed (Zipursky et al. 2007). Future ligand development will likely target other nonmonoaminergic pathophysiologies that are associated with MDD, such as excessive secretion of glucocorticoids, aberrant signal transduction, and markers of cell loss, to increase our understanding of how these pathologies may relate to clinical symptoms and course of illness, and the effects of novel treatments (Meyer 2008).

16.4.3 Drug Addiction

Drug addiction is a disease and is one of the medical consequences of drug abuse.

According to the Diagnostic and Statistical Manual of Mental Disorders (IV), addition is the condition that emerges from chronic drug use that leads to the compulsive administration of the drug despite the fact that the subject may no longer want to take it and even at the expense of seriously adverse consequences.

Abuse of drugs, such as cocaine, methamphetamine, MDMA, alcohol, opiates, tobacco, and marijuana affect genes, protein expression, and neuronal circuits, and engages the neurobiological mechanisms by which nature ensures that behaviors that are indispensable for survival motivate the procurement of more drugs, which can lead to repeated administration and addiction (Volkow 2004).

In the last two decades, PET and SPECT imaging technologies have provided the necessary tools to investigate how genes affect protein expression, how protein expression affects neurobiology, how neurobiology affects behavior, and how that, in turn, affects social interactions.

16.4.3.1 The Brain's Reward System

The brain dopamine system is central to the brain's reward system (BRS) (Fig. 16.41) and a major molecular target in the investigation of drug abuse (Koob and Bloom 1988). The cell bodies of neurons which produce dopamine are located in the substantia nigra and the ventral tegmental area in the midbrain and project to the striatal area that includes, what has come to be known as, the reward center (the nucleus accumbens). Dopamine cells from the midbrain also project to various cortical and limbic brain regions. Typically, drug induced elevations in dopamine occur rapidly after the administration of the drug and are associated with an intense euphoria or "*high.*" Although different drugs act by different

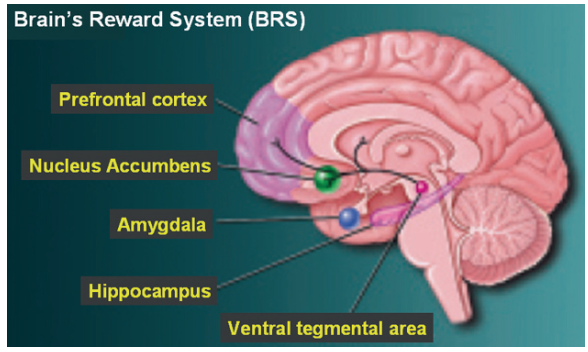

Fig. 16.41 The brain dopamine system is central to the brain's reward system (BRS) and a major molecular target in the investigation of drug abuse

mechanisms, increased levels of synaptic dopamine is common to all of them (Volkow et al. 2003).

Cocaine, a powerful addictive psychostimulant, binds to monoamine (dopamine, norepinephrine, and serotonin) transporters with micromolar to submicromolar affinity. Specifically, dopamine transporter (DAT) blockage results in the elevation of synaptic dopamine (DA) in the nucleus accumbens and the ensuing stimulation of dopamine receptors. However, on the basis of studies with [^{11}C]cocaine, it was observed that the highest density of DAT binding sites for cocaine is in the basal ganglia. Also, on the basis of imaging studies using [^{11}C]cocaine, it was determined that a DAT occupancy in excess of 60% is required to become high (Volkow et al. 2003).

[^{18}F]NMSP, as well as [^{11}C]raclopride (the dopamine D_2 receptor ligands), have been used to measure dopamine D_2 receptors (on the postsynaptic neurons in basal ganglia) in addicted individuals. Prior administration of cocaine (or methylphenidate) blocks DATs and increases the synaptic dopamine levels. The subsequent D_2 receptor imaging studies have clearly demonstrated that the binding of the radiotracer decreases, while the availability of D_2 receptors significantly decreases (Fig. 16.42). Also, PET studies have consistently shown long lasting decreases in dopamine D_2 receptors in cocaine abusers, compared to control subjects (Volkow et al. 2003). Several investigators have also documented dopamine D_2 reductions with alcohol and methamphitamine addictions.

Studies of brain glucose metabolism with FDG-PET in cocaine abusers, during short and long term withdrawal, have demonstrated decreased activity in the anterior cingulate gyrus (CG) and orbitofrontal cortex (OFC), which are both projection areas of the mesolimbic dopamine known to be involved in compulsive behavior (Volkow et al. 1992). The decrease in metabolic activity (CMRglc) in these areas could result in an inability to control the intake of the drug under emotionally stressful situations. During craving, one week after cocaine withdrawl, CMRglc is generally increased, and the intensity of cocaine craving is correlated with increased CMRglc in the prefrontal cortex (PFC) and OFC. Craving may also be associated with increased μ-opioid binding, as demonstrated with [^{11}C] carfenta-nil, in several brain regions of cocaine addicts for several weeks after their last use of cocaine (Zubieta et al. 1996).

Functional neuromaging can be expected to provide the means by which to objectively link behavioral and neurochemical changes and to objectively evaluate drug abuse and treatment. In addition, with the identification of new genes related to addictive behavior, neuro imaging promises to provide a tool for directly translating this knowledge to an evaluation in human subjects.

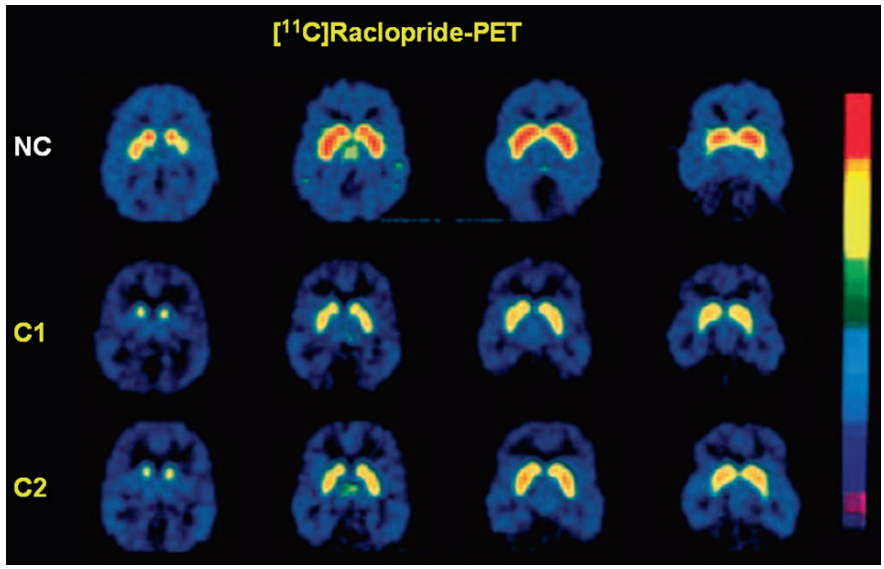

Fig. 16.42 Effect of cocaine abuse on dopamine D_2 receptors. Compared to normal control (NC) subject, [^{11}C] raclopride binding to dopamine receptors in the basal ganglia was significantly decreased in two cocaine abusers; 1 month after cessation of use (C1) and 4 months after cessation of use (C2) (Volkow 2004)

References

Abi-Dargham A, Martinez D, Mawlavi O, et al (2000a) Measurement of striatal and extrastriatal dopamine D1 receptor binding potential with [^{11}C]NNC-112 in humans: validation and reproducibility. J Cereb Blood Flow Metab 20:225–243

Abi-Dargham A, Rodenhiser J, Printz D, et al (2000b) Increased baseline occupancy of D2 receptors by dopamine in schizophrenia. Proc Natl Acad Sci U S A 97(14):8104–8109

Agdeppa ED, Kepe V, Liu J, et al (2001) Binding characteristics of radiofluorinated 6-dialkyl-amino-2-naphtylethylidene derivatives as positron emission tomography imaging probes for β-amyloid plaques in Alzheimer's disease. J Neurosci 21:1–5

Archer HA, Edison P, Brooks DJ, et al (2006) Amyloid load and cerebral atrophy in Alzheimer's disease: an ^{11}C-PIB positron emission tomography study. Ann Neurol 60:145–147

Banati RB, Newcombe J, Gunn RN, et al (2000) The peripheral benzodiazepine binding site in the brain in multiple sclerosis: quantitative in vivo imaging of microglia as a measure of disease activity. Brain 123:2321–2337

Barnes NM, Sharp T (1999) A review of central 5-HT receptors and their function. Neuropharmacology 38:1083–1152

Barrio JR, Huang S-C, Cole G, et al (1999) PET imaging of tangles and plaques in Alzheimer's disease with a highly hydrophobic probe. J Label Compd Radiopharm 42:S194

Bartus RT, Dean RL, Beer B, et al (1982) The cholinergic hypothesis of geriatric memory dysfunction. Science 217:408–17

Belmaker RH, Agam G (2008) Major depressive disorder. N Engl J Med 358:55–68

Bremmer JD, Horti A, Staib LH, et al (2000) Kinetic modeling of benzodiazepine receptor binding with PET and high specific activity [^{11}C]iomazenil in healthy human subjects. Synapse 35:68–77

Blasberg RG, Tjuvajev JG (2003) Molecular-genetic imaging: current and future perspectives. J Clin Invest 111:1620–1629

Bohnen NI, Frey KA (2003) The role of positron emission tomography imaging in movement disorders. Neuroimaging Clin N Am 13:791–803

Boutin H, Chauveau F, Thominiaux C (2007) ^{11}C-DPA-713: a novel peripheral benzodiazepine receptor PET ligand for in vivo imaging of neuroinflammation J Nucl Med 48:573–581

Breier A, Su TP, Saunders R, et al (1997) Schizophrenia is associated with elevated amphetamine-induced synaptic dopamine concentrations: evidence from a novel positron emission tomography method. Proc Natl Acad Sci U S A 94(6):2569–2574

Brooks DJ (2003) PET studies on the function of dopamine in health and Parkinson's disease. Ann N Y Acad Sci 991: 22–35

Brooks DJ (2005) Positron emission tomography and single-photon emission computed tomography in central nervous system drug development. NeuroRx 2:226–236

Buckner RL (2004) Memory and executive function in aging and AD: multiple factors that cause decline and reserve factors that compensate. Neuron 44: 195–208

Casse R, Rowe CC, Newton M, et al (2002) Positron Emission Tomography and Epilepsy Mol Imaging Biol 4:338–351

Chaly T, Dhawan V, Kazumata K, et al (1996) Radiosynthesis of [^{18}F]*N*-3-fluoropropyl-2-β-carbomethoxy-3-β-(4-iodophenyl) nortropane and the first human study with positron emission tomography. Nucl Med Biol 23:999–1004

Chou KL, Hurtig HI, Stern MB, et al (2004) Diagnostic accuracy of [^{99m}Tc]TRODAT-1 SPECT imaging in early Parkinson's disease. Parkinsonism Relat Disord 10:375–379

Crone C (1964) Permeability of capillaries in various organs as determined by the use of indicator diffusion method. Acta Physiol Scand 58:292–305

Cunningham VJ, Gunn RN, Matthews JC (2004) Quantification in positron emission tomography for research in pharmacology and drug development. Nucl Med Commun 25: 643–646

Davis MR, Votaw JR, Bremner JD, et al (2003) Initial human PET imaging studies with the dopamine transporter ligand ^{18}F-FECNT. J Nucl Med 44:855– 861

Dickson DW (1997) The pathogenesis of senile plaques. J Neuropathol Exp Neurol 56:321–339

Diksic M, Tohyama Y, Takada A (2000) Brain net unidirectional uptake of α-methyltryptophan. Neurochem Res 25: 1537–1546

Ding YS, Fowler J (2005) New-generation radiotracers for nAChR and NET. Nucl Med Biol 32:707–718

Ding Y-S, Fowler JS, Volkow ND, et al (1994) Pharmacokinetics and in vivo specificity of [^{11}C]DL-threo-methylphenydate for the presynaptic dopaminergic neuron. Synapse 18: 152–160

Ding Y-S, Volkow ND, Logan J, et al (2000) Occupancy of brain nicotinic acetylcholine receptors by nicotine doses equivalent to those obtained when smoking a cigarette. Synapse 35:234–237

Drzezga A (2008) Basic pathologies of neurodegenerative dementias and their relevance for state-of-the-art molecular imaging studies. Eur J Nucl Med Mol Imaging 35:S4–S11

Eckelman WC (2001) Radiolabeled muscarinic radioligands for in vivo studies. Nucl Med Biol 28:485–491

Eckelman WC, Grissom M, Conklin J, et al (1984) In vivo competition studies with analogues of quinucidinylbenzilate. J Pharm Sci 73:529–533

Eckert T, Eidelberg D (2005) Neuroimaging and therapeutics in movement disorders. NeuroRx 2:361–371

Eshuis SA, Maguire RP, Leenders KL, et al (2006) Comparison of FP-CIT SPECT with FDOPA- PET in patients with de novo and advanced Parkinson's disease. Eur J Nucl Med Mol Imaging 33:200–209

Farde L, Ehrin E, Eriksson L, et al (1985) Substituted benzamides as ligands for visualization of dopamine receptor binding in the human brain by positron emission tomography. Proc Natl Acad Sci U S A 82:3863–3867

Farde L, Wiesel FA, Halldin C, et al (1988) Central D2-dopamine receptor occupancy in schizophrenic patients treated with antipsychotic drugs. Arch Gen Psychiatry 45(1):71–76

Farde L, Nordstrom AL, Wiesel FA, et al (1992) Positron emission tomographic analysis of central D1 and D2 dopamine receptor occupancy in patients treated with classical neuroleptics and clozapine: relation to extrapyramidal side effects. Arch Gen Psychiatry 49:538–544

Firnau G, Sood S, Chirakal R, et al (1988) Metabolites of 6-[^{18}F] fluoro-L-dopa in human blood. J Nucl Med 29:363–369

Fischman AJ, Bonab AA, Babich JW, et al (2001) [^{11}C, ^{127}I] Altropane: a highly selective ligand for PET imaging of dopamine transporter sites. Synapse 39:332–342

Fischman AJ (2005) Role of [^{18}F]-dopa–PET imaging in assessing movement disorders. Radiol Clin N Am 43:93–106

Fowler JS, MacGregor RR, Wolf AP, et al (1987a) Mapping human brain monoamine oxidase A and B with ^{11}C-suicide inactivators and positron emission tomography. Science 235:481–485

Fowler JS, Volkow ND, Wolf AP, et al (1987b) Mapping cocaine binding in human and baboon brain in vivo. Synapse 4:371–377

Fowler JS, Volkow ND, Wang G-J, et al (1996) Inhibition of monoamine oxidase B in the brains of smokers. Nature 379:733–736

Fowler JS, Ding Y-S, Volkow ND (2003) Radiotracers for Positron Emission Tomography Imaging. Semi Nucl Med 33:14–27

Frackowiak RS, Lenzi GL, Jones T, et al (1980) Quantitative measurement of regional cerebral blood flow and oxygen metabolism in man ^{15}O and positron emission tomography: theory, procedure and normal values. J Comput Assisted Tomogr 4:727–736

Frankle WG, Laruelle M (2002) Neuroreceptor imaging in psychiatric disorders. Ann Nucl Med 16(7):437–446

Frey KA, Koeppe RA, Kilbourn MR, et al (1996) Presynaptic monoaminergic vesicles in Parkinson's disease and normal aging. Ann Neurol 40:873–884

Frey KA, Koeppe RA, Kilbourn MR (2001) Imaging the vesicular monoamine transporter. Adv Neurol 86:237–247

Frost JJ (2001) PET imaging of the opioid receptor. The early years. Nucl Med Biol 28:509–513

Frost JJ, Wagner Henry JJ, Danals RF, et al (1985) Imaging opiate receptors in the human brain by positron emission tomography. J Comput Asstisted Tomogr 9:231–236

Garnett ES, Firnau G, Nahmias C (1983) Dopamine visualized in the basal ganglia in living human brain. Nature 305–137–138

Garnett ES, Nahmias C, Firnau G (1984) Central dopaminergic pathways in hemiparkinsonism examined by positron emission tomography. Can J Neurol Sci 11:174–179

Gibb AJ. Neurotransmitter receptors. In: Webster RA, ed. Neurotransmitters, drugs and brain function. Wiley, New York, NY, pp 57–79

Gilman S, Koeppe RA, Junck L, et al (1995) Benzodiazepine receptor binding in cerebellar degenerations studied with positron emission tomography. Ann Neurol 38:176–185

Ginovart N, Wilson AA, Meyer JH, et al (2003) [^{11}C]-DASB, a tool for in vivo measurement of SSRI-induced occupancy of the serotonin transporter: PET characterization and evaluation in cats. Synapse 47:123–133

Goffin K, Dedeurwaerdere S, Van Laere K, et al (2008) Neuronuclear assessment of patients with epilepsy. Semin Nucl Med 38:227–239

Gulyas B, Halldin C, Sandell J, et al (2002) PET studies on the brain uptake and regional distribution of [^{11}C]vinpocetine in human subjects. Acta Neurol Scand 106:325–332

Halldin C, Farde L, Hogberg T, et al (1995) Carbon-11-FLB 457: a radioligand for extra-striatal D_2 dopamine receptors. J Nucl Med 36:1275–1281

Hammoud DA, Endres CJ, Chander AR, et al (2005) Imaging glial cell activation with [^{11}C]-R-PK11195 in patients with AIDS. J Neurovirol 11:346–355

Hammoud DA, Hoffman JM, Pomper MG (2007) Molecular neuroimaging: from conventional to emerging techniques. Radiology 245:21–42

Harpstrite SE, Prior J, Piwnica-Worms D, et al (2005) Peptide conjugates for imaging-amyloid in the brain. J Label Compd Radiopharm 48(s1):S228

Henriksen G, Yousefi BH, Drzezga A, et al (2008) Development and evaluation of compounds for imaging of β-amyloid plaque by means of positron emission tomography. Eur J Nucl Med Mol Imaging 35(Suppl 1):S75–S81

Herscovitch P, Markham J, Raichle ME (1983) Brain blood flow measured with intravenous [^{15}O] water, I: theory and error analysis. J Nucl Med 24:782–789

Heiss WD, Herholz K (2006) Brain receptor imaging. J Nucl Med 47:302–312

Herholz K (2008) Acetylcholine esterase activity in mild cognitive impairment and Alzheimer's disease. Eur J Nucl Med Mol Imaging 35(Suppl 1):S25–S29

Herholz K, Heiss WD (2004) Positron emission tomography in clinical neurology. Mol Imaging Biol 6:239–269

Herholz K, Herscovitch P, Heiss W-D (2004). NeuroPET. Springer, Berlin

Holman BL, Gibson RE, Hill TC, et al (1985) Muscarinic acetylcholine receptors in Alzheimer's disease: in vivo imaging with iodine 123-labeled 3-quinuclidinyl-4-iodobenzilate and emission tomography. JAMA 254:3063–3066

Hume SP, Gunn RN, Jones T (1998) Pharmacological constraints associated with positron emission tomographic scanning of small laboratory animals. Eur J Nucl Med 25:173–176

Hustinx R, Pourdehnad M, Kaschten B, Alavi A (2005) PET imaging for differentiating recurrent brain tumor from radiation necrosis Radiol Clin North Am 43:35–47

Jack CR Jr, Lowe VJ, Senjem ML, et al (2008) ^{11}C PIB and structural MRI provide complementary information in imaging of Alzheimer's disease and amnestic mild cognitive impairment. Brain 131:665–680

Jacobs A, Voges J, Reszka R, et al (2001) Positron-emission tomography of vector mediated gene expression in gene therapy for gliomas. Lancet 358:727–729

Jacobs AH, Li H, Winkeler A, et al (2003) PET-based molecular imaging in neuroscience Eur J Nucl Med Mol Imaging 30:1051–1065

Jacobs AH, Winkler A, Castro MG, et al (2005) Human gene therapy and imaging in neurological diseases. Eur J Nucl Med Mol Imag 32:S358–S383

Jagust W (2004) Molecular neuroimaging in Alzheimer's disease. Neuro Rx 1:206–212

Jennings DL, Seibyl JP, Oakes D, et al (2004) (^{123}I) beta-CIT and single photon emission computed tomographic imaging vs clinical evaluation in Parkinsonian syndrome: unmasking an early diagnosis. Arch Neurol 61:1224–1229

Jones T, Chesler DA, Ter-Pogossian MM, et al (1976) The continuous inhalation of oxygen-15 for assessing regional oxygen extraction in the brain of man. Br J Radiol 49:339–343

Juhasz C, Chugani HT (2003) Imaging the epileptic brain with positron emission tomography. Neuroimaging Clin N Am 13:705–716

Kapur S, Remington G (2001) Dopamine D_2 receptors and their role in atypical antipsychotic action: still necessary and may even be sufficient. Biol Psychiatry 50(11):873–883

Kapur S, Zipursky R, Jones C, et al (2000) A positron emission tomography study of quetiapine in schizophrenia: a preliminary finding of an antipsychotic effect with only transiently

high dopamine D2 receptor occupancy. Arch Gen Psychiatry 57:553–559

Kato H, Shimosegawar E, Oku N, et al (2008) MRI-based correction for partial-volume effect improves detectability of intractable epileptogenic foci on 123I-Iomazenil brain SPECT images. J Nucl Med 49:383–389

Kauppinen T, Bergstrom K, Heikman P, et al (2003) Biodistribution and radiation dosimetry of [^{123}1]ADAM in healthy human subjects: preliminary results. Eur J Nucl Med 30:132–136

Kemppainen NM, Aalto S, Wilson IA, et al (2007) PET amyloid ligand [^{11}C]PIB uptake is increased in mild cognitive impairment. Neurology 68:1603–1606

Kirik D, Breysse N, Björklund T (2005) Imaging in cell-based therapy for neurodegenerative diseases. Eur J Nucl Med Mol Imaging 32:S417–S434

Kling MA, Carson RE, Borg L, et al (2000) Opioid rceptor imaging with positron emission tomography and [^{18}F]cyclofoxy in long-term, methadone-treated former heroin addicts. J Pharm Exp Ther 295:1070–1076

Klunk WE, Wang Y, Huang G-F (2003) The binding of 2-(4′-ethylaminophenyl)benzothiazole to postmortem brain homogenates is dominated by the amyloid component. J Neurosci 23(6):2086–2092

Klunk WE, Engler H, Nordberg A, et al (2004) Imaging brain amyloid in Alzheimer's disease with Pittsburgh compound-B. Ann Neurol 55:306–319

Koeppe RA, Frey KA, Snyder SE, et al (1999) Kinetic modeling of N-[^{11}C]methylpiperidin-4-yl propionate: alternatives for analysis of an irreversible positron emission tomography tracer for measurement of acetylcholinesterase activity in human brain. J Cereb Blood Flow Metab19:1150–1163

Koob GF, Bloom FE (1988) Cellular and molecular mechanisms of drug dependence. Science 242:715–723

Kudo Y, Okamura N, Furumoto S, et al (2007) 2-(2-[2-Dimethylaminothiazol-5-yl]Ethenyl)-6-(2-[Fluoro]Ethoxy) Benzoxazole: a novel PET agent for in vivo detection of dense amyloid plaques in Alzheimer's disease patients. J Nucl Med 48:553–561

Kuhl DE, Koeppe RA, Minoshima S, et al (1999) In vivo mapping of cerebral acetylcholinesterase activity in aging and Alzheimer's disease. Neurology 52:691–699

Kuhl DE, Minoshima S, Frey KA, et al. (2000) Limited donepezil inhibition of acetylcholinesterase measured with positron emission tomography in living Alzheimer cerebral cortex. Ann Neurol. 48:391–395

Kulak JM, Sum J, Musachio JL, et al (2002): 5-Iodo-A-85380 binds to alpha-conotoxin MII-sensitive nicotinic acetylcholine receptors (nAChRs) as well as alpha4beta2* subtypes. J Neurochem 81:403–406

Kung HF, Kung M-P, Choi SR (2003a) Radiopharmaceuticals for single-photon emission computed tomography brain imaging. Semin Nucl Med 33:2–13

Kung HF, Kung M-P, Zhuang ZP, (2003b) Iodinated tracers for imaging amyloid plaques in the brain. Mol Imaging Biol 5:418–426

Kumar A, et al (2003) Brain 126:2648–2655

Laruelle M, Abi-Dargham A, van Dyck CH, et al (1996) Single photon emission computerized tomography imaging of amphetamine-induced dopamine release in drug-free schizophrenic subjects. Proc Natl Acad Sci U S A 93(17):9235–9240

Laruelle M, Talbot P, Martinez D, et al (2002) Psychiatric disorders. In: Wahl RL (ed) Principles and Practice of positron emission tomography, Lippincott Williams & Wilkins, Philadelphia

Ma Y, Dhawan V, Mentis M, Chaly T, et al (2002) Parametric mapping of [18F]FPCIT binding in early stage Parkinson's disease: a PET study. Synapse 45:125–133

Ma B, Sherman PS, Moskwa JE, et al (2004) Sensitivity of [^{11}C] N-methylpyrroli-dinyl benzilate ([^{11}C]NMPYB) to endogenous acetylcholine: PET imaging vs tissue sampling methods. Nucl Med Biol 31:393–397

Machulla H-J, Heinz A (2005) Radioligands for brain imaging of the κ-opioid system. J Nucl Med 46:386–387

Maeda J, Suhara T, Zhang MR, et al (2004) Novel peripheral benzodiazepine receptor ligand [^{11}C]DAA1106 for PET: an imaging tool for glial cells in the brain. Synapse 52:283–291

Mahley RW, Weisgraber KH, Huang Y (2006) Apolipoprotein E4: a causative factor and therapeutic target in neuropathology, including Alzheimer's disease. Proc Natl Acad Sci U S A 103:5644–5651

Markus R, Donnan GA, Kazui S, et al (2002) Statistical parametric mapping of hypoxic tissue identified by [^{18}F] fluoromisonidazole and positron emission tomography following acute ischemic stroke. Neuroimage 16:425–433

Marshall V, Grosse D (2003) Role of dopamine transporter imaging in routine clinical practice. Mov Disord 18:1415–1423

Massoud TF, Gambhir SS (2003) Molecular imaging in living subjects: seeing fundamental biological processes in a new light. Genes Dev 17:545–580

Mathis CA, Bacskai BJ, Kajdasz ST, et al (2002) A lipophilic thioflavin-T derivative for positron emission tomography (PET) imaging of amyloid in brain. Bioorg Med Chem Lett 12:295–298

Mathis CA, Wang Y, Klunk WE (2004) Imaging beta-amyloid plaques and neurofibrillary tangles in the aging human brain. Curr Pharm Des 10:1469–1492

Mathis CA, Loprestia BJ, Klunk WE (2007) Impact of amyloid imaging on drug development in Alzheimer's disease. Nucl Med Biol 34:809–822

Mazziotta JC, Phelps ME, Miller J (1981) Tomographic mapping of human cerebral metabolism. Neurology 31:503–516

Meltzer CC, Cantwell MN, Greer PJ, et al (2000) Does cerebral blood flow decline in healthy aging? A PET study with partial volume correction. J Nucl Med 41:1842–1848

Merlet I, Ostrowsky K, Costes N, et al (2004) 5-HT_{1A} receptor binding and intracerebral activity in temporal lobe epilepsy: an [^{18}F]MPPF-PET study. Brain 127:900–913

Meyer JH (2008) Applying neuroimaging ligands to study major depressive disorder. Semin Nucl Med 38:287–304

Meyer J, Kapur S, Houle S, et al (1999) Prefrontal cortex 5-HT2 receptors in depression: a [18F]setoperone PET imaging study. Am J Psychiatry 156(7):1029–1034

Meyer JH, Kruger S, Wilson AA, et al (2001a) Lower dopamine transporter binding potential in striatum during depression. Neuroreport 12(18):4121–4125

Meyer JH, Wilson AA, Ginovart N, et al (2001b) Occupancy of serotonin transporters by paroxetine and citalopram during treatment of depression: a [(11)C]DASB PET imaging study. Am J Psychiatry 158(11):1843–1849

Meyer JH, McMain S, Kennedy SH, et al (2003) Dysfunctional attitudes and 5-HT(2) receptors during depression and self-harm. Am J Psychiatry 160(1):90–99

Meyer JH, Wilson AA, Sagrati S, et al (2004) Serotonin transporter occupancy of five selective serotonin reuptake inhibitors at

different doses: an [11C]DASB positron emission tomography study. Am J Psychiatry 161(5):826–835
Mintun MA, Larossa GN, Sheline YI, et al (2006) [11C]PIB in a nondemented population: potential antecedent marker of Alzheimer disease. Neurology 67:446–452
Morris JH, Nagy Z (2004) Alzheimer's disease. In: Esiri MM, Lee VM, Trojanowski JQ (eds) The neuropathology of dementia, 2nd edn. Cambridge University Press, Cambridge, UK
Mozley PD, Schneider JS, Acton PD, et al (2000) Binding of 99mTc-TRODAT-1 to dopamine transporters in patients with Parkinson's disease and in healthy volunteers. J Nucl Med 41:584–589
Mukherjee J, Kang ZY, Brown T, et al (1999) Preliminary assessment of extrastriatal dopamine D2 receptor binding in the rodent and nonhuman primate brains using the high affinity radioligand, 18F-Fallypride. Nucl Med Biol 26:519–527
Newberg AB, Alavi A (2005) PET in seizure disorders. Radiol Clin North Am 43:79–92
Ng S, Villemagne VL, Berlangieri S, et al (2007) Visual assessment versus quantitative assessment of [11C]PIB PET and [18F]FDG PET for detection of Alzheimer's disease. J Nucl Med 48:547–552
Nordberg A (2008) Amyloid plaque imaging in vivo: current achievement and future prospects. Eur J Nucl Med Mol Imaging 35:S46–S50
Parsey RV, Mann JJ (2003) Applications of positron emission tomography in psychiatry. Semin Nucl Med 33(2):129–135
Pappata S, Tavitian B, Traykov L, et al (1996) In vivo imaging of human cerebral acetylcholinesterase. J Neurochem 67:876–879
Passchier J, van Waarde A (2001) Visualization of serotonin-1A (5-HT1A) receptors in the central nervous system. Eur J Nucl Med 28:113–129
Passchier J, van Waarde A, Pieterman RM, et al (2000) In vivo delineation of 5-HT1A receptors in human brain with [18F] MPPF. J Nucl Med 41:1830–1835
Persson A, Ehrin E, Eriksson, et al (1985) [11C]Ro-15–1788 binding to benzodiazepine receptors in the human brain by positron emission tomography. J Psychiatry Res 19: 609–622
Petrella JR, Mattay VS, Doraiswamy PM (2008) Imaging genetics of brain longevity and mental wellness: the next frontier? Radiology:246:20–32
Podruchny TA, Connolly C, Bokde A, et al (2003) In vivo muscarinic 2 receptor imaging in cognitively normal young and older volunteers. Synapse 48:39–44
Price JL (1997) Diagnostic criteria for Alzheimer's disease. Neurobiol Aging 18:S67–S70
Phelps ME, Huang SC, Hoffman EJ, et al (1979) Tomographic measurement of local cerebral glucose metabolic rate in human with [18F]2-fluoro-2-deoxyglucose. Validation of method. Ann Neurol 6:371–388
Pike VW (1995) Radioligands for PET studies of central 5-HT receptors and re-uptake sites- current status. Nucl Med Biol 22:1011–1018
Pike KE, Savage G, Villemagne VL, et al (2007) β-amyloid imaging and memory in non-demented individuals: evidence for preclinical Alzheimer's disease. Brain 130:2837–2844
Raichle ME, Martin WRW, Herscovitch P, et al (1983) Brain blood flow measured with intravenous $H_2{}^{15}O$. II. Implementation and validation. J Nucl Med 24:790–798
Ravina B, Eidelberg D, Ahlskog JE, et al (2005) The role of radiotracer imaging in Parkinson disease. Neurology 64:208–215
Read SJ, Hirano T, Abbott DF, et al (1998) Identifying hypoxic tissue after acute ischemic stroke using PET and 18F-fluoromisonidazole. Neurology 51:1617–1621
Reiman EM, Chen K, Alexander GE, et al (2004) Functional brain abnormalities in young adults at genetic risk for late-onset Alzheimer's dementia. Proc Natl Acad Sci U S A 101:284–289
Reivich N, Kuhl D, Wolf A, et al (1979) The [18F] Fluorodeoxyglucose method for the measurement of local cerebral glucose utilization in man. Circ Res 44:127–137
Robeson W, Dhawan V, Belakhlef A, et al. (2003) Dosimetry of the dopamine transporter radioligand 18F-FPCIT in human subjects. J Nucl Med 44:961–966
Rosas HD, Feigin AS, Hersch SM (2004) Using advances in neuroimaging to detect, understand, and monitor disease progression in Huntington's disease. NeuroRx 1:263–272
Rowe CC, Ng S, Ackermann U, et al (2007) Imaging beta-amyloid burden in aging and dementia. Neurology 68:1718–1725
Rowe CC, Ackerman U, Browne W, et al (2008) Imaging of amyloid β in Alzheimer's disease with 18F-BAY94–9172, a novel PET tracer: proof of mechanism. Lancet Neurol 7:129–35
Ryzhikov NN, et al (2005) Preparation of highly specific radioactivity [18F]flumazenil and its evaluation in cynomolgus monkey by positron emission tomography. Nucl Med Biol 32:109–116
Sabri O, Kendziorra K, Wolf H, et al (2008) Acetylcholine receptors in dementia and mild cognitive impairment. Eur J Nucl Med Mol Imaging 35(s1):S30–S45
Saur D, Buchert R, Knab R, et al (2006) Iomazenil-single-photon emission computed tomography reveals selective neuronal loss in magnetic resonance-defined mismatch areas. Stroke 37:2713–2719
Seibyl JP (2008) Single-photon emission computed tomography and positron emission tomography evaluations of patients with central motor disorders. Semin Nucl Med 38:274–286
Selleri S, Bruni F, Costagli C, et al (2001) 2-Arylpyrazolo[1,5-a] pyrimidin-3-yl acetamides: new potent and selective peripheral benzodiazepine receptor ligands. Bioorg Med Chem 9:2661–2671
Shiue C-Y, Welch MJ (2004) Update on PET radiopharmaceuticals: life beyond fluorodeoxyglucose. Radiol Clin N Am 42:1033–1053
Shoghi-Jadid K, Small GW, Agdeppa ED, et al (2002) Localization of neurofibrillary tangles and beta-amyloid plaques in the brains of living patients with Alzheimer disease. Am J Geriatr Psychiatry 10:24–35
Siesjo BK (1978) Brain energy metabolism. Wiley, New York, pp 101–110
Silverman DHS (2004) Brain 18F-FDG PET in the diagnosis of neurodegenerative dementias: comparison with perfusion SPECT and with clinical evaluations lacking nuclear imaging. J Nucl Med 45:594–607
Silverman DHS, Mosconi L, Ercoli L, et al (2008) Positron emission tomography scans obtained for the evaluation of cognitive dysfunction. Semin Nucl Med 38:251–261
Small GW, Kepe V, Ercoli LM, et al (2006) PET of brain amyloid and tau in mild cognitive impairment. N Engl J Med 355:2652–2663

Smith GS, Koppel J, Goldberg S (2003) Applications of neuroreceptor imaging to psychiatry research. Psychopharmacol Bull 37:26–65

Suhara T, Maeda J, Kawabe K, et al (2003a) Visualization of alpha5 subunit of GABAA/benzodiazepine receptor by [^{11}C] Ro15–4513 using positron emission tomography. Synapse 47:200–208

Suhara T, Takano A, Sudo Y, et al (2003b) High levels of serotonin transporter occupancy with low-dose clomipramine in comparative occupancy study with fluvoxamine using positron emission tomography. Arch Gen Psychiatry 60(4):386–391

Sullivan JP, DonnellyRD, Briggs CA, et al (1996) A-85380 [3-(2(*S*)-azetidinylmethoxy)-pyridine]: in vitro pharmacological properties of a novel, high affinity α4β2 nicotinic acetylcholine receptor ligand. Neuropharmacology 35:725–734

Szelies B, Sobesky J, Pawlik G, et al (2002) Impaired benzodiazepine receptor binding in peri-lesional cortex of patients with symptomatic epilepsies studies by [C-11]-flumazenil PET. Eur J Neurol 9:137–142

Talbot PS, Narendran R, Butelman ER, et al (2005) [^{11}C] GR103545, a radiotracer for imaging κ-opioid receptors in vivo with PET: synthesis and evaluation in baboons J Nucl Med 46:484–494

Ter-Pogossian MM, Eichling JO, Davis DO, et al (1969) The determination of regional cerebral blood flow by means of water labeled with radioactive oxygen-15. J Clin Invest 93:31–40

Theodore WH (2004) Recent advances and trends in epilepsy imaging: pathogenesis and pathophysiology. Rev Neurol Dis 1(2):53–59

Thominiaux C, Dolle F, James ML, et al (2006) Improved synthesis of the peripheral benzodiazepine receptor ligand [^{11}C] DPA-713 using [^{11}C]methyl triflate. Appl Radiat Isot 64:570–573

Toczek MT, Carson RE, Lang L, et al (2003) PET imaging of 5-HT1A receptor binding in patients with temporal lobe epilepsy. Neurology 60:749–756

Toyama H, Ye D, Ichise M, et al (2005) PET imaging of brain with the beta-amyloid probe, [^{11}C]6-OH-BTA-1, in a transgenic mouse model of Alzheimer's disease. Eur J Nucl Med Mol Imaging 32:593–600

Treiman DM (2001) GABAergic mechanisms in epilepsy. Epilepsia 42(Suppl 3):8–12

Vallabhajosula S, Hirschowitz J, Machac J (1997) Effect of haloperidol dose on ^{123}I-IBZM brain SPECT imaging in schizophrenic patients. J Nucl Med 38:203–207

Verhoeff NP, Wilson AA, Takeshita S, et al (2004) In-vivo imaging of Alzheimer disease beta-amyloid with [^{11}C]SB-13 PET. Am J Geriatr Psychiatry 12:584–595

Volkow ND (2004) Imaging the addicted brain: from molecules to behavior. J Nucl Med 45:(11):13N–24N

Volkow ND, Hitzemann R, Wang GJ, et al (1992) Long-term frontal brain metabolic changes in cocaine dependence and withdrawal. Am J Psychiatry 148:621–626

Volkow ND, Fowler JS, Gatley SJ, et al (1996) PET evaluation of dopamine system of the human brain. J Nucl Med 37:1242–1256

Volkow ND, Fowler JS, Wang G-J (2003) Positron emission tomography and single-photon emission computed tomography in substance abuse research. Semin Nucl Med 34(2):114–128

Waarde A (2000) Measuring receptor occupancy with PET. Curr Pharm Des 6:1593–1610

Wagner HN Jr, Burns HD, Dannals RF, et al (1983) Imaging dopamine receptors in the human brain by positron tomography. Science 221:1264–1266

Wang J, Dickson DW, Trojanowski JQ, et al (1999) The levels of soluble versus insoluble brain Aβ distinguish Alzheimer's disease from normal and pathologic aging. Exp Neurol 158:328–337

Wang J, Zuo C-T, Jiang Y-P, et al (2006) ^{18}F-FP-CIT PET imaging and SPM analysis of dopamine transporters in Parkinson's disease in various Hoehn & Yahr stages. J Neurol 254:185–190

Webster R (2001) Neurotransmitter systems and function: overview. In: Webster RA, (ed) Neurotransmitters, drugs and brain function. Wiley, New York, NY, pp 1–32

Webster R (2001) Other transmitters and mediators. In: Webster RA, ed. Neurotransmitters, drugs and brain function. Wiley, New York, NY, pp 265–286

Whiteman M, Armstrong JS, Chu SH, et al (2004) The novel neuromodulator hydrogen sulfide: an endogenous peroxynitrite "scavenger"? J Neurochem 90:765–768

Wintermark M, Albers GW, Alexandrov AV (2008) Acute stroke imaging research roadmap. Am J Neuroradiol 29:E23–E30

Zhang MR, Maeda J, Ogawa M, et al (2004) Development of a new radioligand, N-(5-fluoro-2-phenoxyphenyl)-N-(2-[$_{18}$F] fluoroethyl-5-methoxybenzyl)acetamide, for PET imaging of peripheral benzodiazepine receptor in primate brain. J Med Chem 47:2228–2235

Zhang W, Oya S, Kung MP, et al (2005a) F-18 stilbenes as PET imaging agents for detecting beta-amyloid plaques in the brain. J Med Chem 48: 5980–88

Zhang W, Oya S, Kung MP, et al (2005b) F-18 polyethyleneglycol stilbenes as PET imaging agents targeting A beta aggregates in the brain. Nucl Med Biol 32: 799–809

Zipursky RB, Meyer JH, Verhoeff NP (2007) PET and SPECT imaging in psychiatric disorders. Can J Psychiatry 52: 146–157

Zoghbi SS, Shetty HU, Ichise M, et al (2006) ^{18}F-FECNT: a polar radiometabolite confounds brain radioligand measurements. J Nucl Med 47:520–527

Zubieta JK, Gorelick DA, Stauffer R, et al (1996) Increased μ-opioid receptor binding detected by PET in cocaine-dependent men is associated with cocaine craving. Nat Med 2:1225–1229